

Assessment of Residual Composite Properties as Influenced by Thermal Mechanical Aging

by

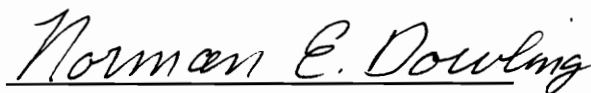
Richard Plunkett

Thesis submitted to the Faculty of the
Virginia Polytechnic Institute and State University
in partial fulfillment of the requirements for the degree of
Master of Science
in
Engineering Mechanics

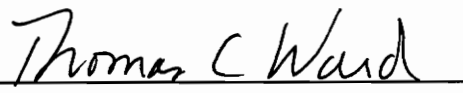
APPROVED:



John J. Lesko, Chairman



Norman E. Dowling



Thomas C. Ward

October, 1996

Blacksburg, Virginia

Key Words: Thermal, Mechanical, Aging, Composite, IITRI, Compression,
DSC, TGA

C.2

LD
5655
V855
1996
PS86
C.2

Assessment of Residual Composite Properties as Influenced by Thermal Mechanical Aging

by

Richard B. Plunkett

John J. Lesko, Chairman

Engineering Mechanics

(ABSTRACT)

In this study, two quasi-isotropic carbon fiber-reinforced polyimide material systems, IM7/K3B and IM7/PETI-5, were thermally aged at 163°C for up to 3000 hours under a static compressive load. The future goal of this study is to determine the effect of 10,000 hours (currently underway) and possibly seven years of aging on these materials. The compressive load was applied using steel fixtures supplied by The Boeing Company. Back-to-back gages on the aging panels monitored compressive strain as well as bending strain. Following aging at 1500 and 3000 hours, ambient residual compression properties were assessed using the IITRI compression test method. Unexposed specimens were also tested to obtain baseline properties for comparison. These results showed that 3000 hours of stressed isothermal aging did not significantly affect the compressive properties of the two composite systems. A slight increase in scatter of the residual strength numbers was observed. Statistical evaluation of the results was used to compute design allowables and quantify changes in scatter.

Differential scanning calorimetry (DSC) was used to monitor any changes in glass transition temperature as a result of the aging. Only small changes were observed in the

DSC scans. Dynamic thermogravimetric analysis (TGA) tests were used to compare weight loss rate versus temperature results for the different age materials. Results show different rates of degradation occurring in the different K3B polymer aging histories. In addition to establishing the effect of isothermal aging under load on the compressive moduli and strength of two polymer-matrix composites, this experiment links increasing scatter in residual strength measurements to changing thermogravimetric results.

ACKNOWLEDGMENTS

The author would like to thank the following people for their contribution to this work:

- Dr. J. J. Lesko, for all of the time and effort he spent as advisor and committee chairman to this project. His ideas and advice contributed greatly to this work's development.
- Dr. T. C. Ward and Dr. N. E. Dowling, for serving as committee members and for helping to edit this document.
- Dr. P. H. Tsang, for his help in preparing the aging setup and straining the panels.
- Dr. J. D. Wood, for her help with experimental details and for her photomechanics expertise which may prove to be very useful for elevated temperature strain measurements.
- Carrie Case, for her assistance in completing the statistical analysis of the compression data.
- The Boeing Company and NASA, for funding this work and supplying the author with material systems, and Antonio Rufin for supervising this work and for taking the time to answer any and all of the author's questions.

- Mark Muggli, for introducing the author to dilatometry and for helping to interpret the DSC data.
- Dr. S. V. Davis, for introducing the author to the DSC and TGA equipment and for helping to interpret their results.
- Dr. S. W. Case and members of the MRG for their friendship and assistance in whatever was asked of them.
- Dr. H. L. McMannus and Ronan Cunningham, for answering the authors questions concerning TGA modeling.
- Bill Shaver and Archie Montgomery, for grinding and cutting all of the panels into precise specimens required for the compression tests.
- Bob Simonds, for his assistance in setting up the compression tests and for providing any necessary equipment.
- Danny Reed, for his help sandblasting.
- The MRG Staff, Shelia Collins, Paula Lee and Cindy Hopkins, for all of their help.
- Mr. and Mrs. Plunkett, the authors parents, for many years of encouragement and support.
- Sarah Adams, my best friend and lay-reader whose patience and understanding over the past months has been phenomenal.

TABLE OF CONTENTS

LIST OF TABLES ix

LIST OF FIGURES x

I. INTRODUCTION 1

Literature Review 2

Aging 2

Physical and Chemical Aging 2

DSC and TGA 6

Compression Tests 8

Summary 10

Problem Statement 11

II. EXPERIMENTAL PROCEDURES 12

Material 12

Environmental Conditioning 13

Specimen Preparation 20

Compression Tests 20

DSC and TGA 23

Mechanical Tests 25

IITRI Compression 25

Differential Scanning Calorimetry 25

Thermogravimetric Analysis 28

III. EXPERIMENTAL RESULTS AND DISCUSSION 29

Applied Aging Strain 29

3000-Hour Panels 29

Thermal Compensation 38

1500-Hour Panels 43

Compression Tests 48

Statistical Analysis 52

Differential Scanning Calorimetry 60

Thermogravimetric Analysis 70

IV. SUMMARY AND CONCLUSIONS 79

Summary of Experimental Procedures 79

Material 79

Environmental Conditioning 80

Specimen Preparation 80

Mechanical Tests 80

Summary of Experimental Results and Discussion 81

Applied Aging Strain 81

3000-Hour Panels 81

1500-Hour Panels 82

Compression Tests 82

Statistical Analysis 82

Differential Scanning Calorimetry 83

Thermogravimetric Analysis 83

Future Recommendations 84

REFERENCES 86

APPENDIX A 89

Panel-Fixture Thermal Expansion Model 89

Weibull Equations 91

VITA 93

LIST OF TABLES

Table 1. Slope of the strain decline in the compressed panels with aging time	33
Table 2. IITRI compression results for the IM7/K3B composite	55
Table 3. IITRI compression results for the IM7/PETI-5 composite	56
Table 4. Weibull statistics for the IM7/PETI-5 composite	58
Table 5. Weibull statistics for the IM7/K3B composite	59
Table 6. Glass transition temperature as determined by DSC	63
Table 7. TGA results for the IM7/K3B composite	73
Table 8. TGA results for the IM7/PETI-5 composite	74

LIST OF FIGURES

Figure 1.	Loading fixture (Drawing courtesy of Boeing)	14
Figure 2.	Loading fixture (panel edge view)	16
Figure 3.	Straining and aging setup for the panel-fixture assemblies	17
Figure 4.	Blue M aging oven containing the sixteen aging fixtures	19
Figure 5.	Tabbing fixture and tabbed composite panel	21
Figure 6.	Specimen sketch (a) top view (b) edge view and close-up photograph of a tabbed specimen (edge view) displaying a typical spew angle	22
Figure 7.	Wired IITRI specimen aligned in the grips	24
Figure 8.	IITRI compression fixture diagram (ASTM)	26
Figure 9.	IITRI compression fixture and gripped specimen	27
Figure 10.	Average panel and rod strains for the IM7/K3B material aged for 3000 hours	30
Figure 11.	Average panel and rod strains for the IM7/PETI-5 material aged for 3000 hours	31
Figure 12.	Three year strain history for initially applied strains of $\pm 780\mu\epsilon$	35
Figure 13.	Three year strain history for initially applied strains of $\pm 1350\mu\epsilon$	36
Figure 14.	Three year strain history for the unloaded specimens	37
Figure 15.	Theorized effects of strain gage adhesive creep and gage foil corrosion on measured electrical strain (Shay)	39

Figure 16. Panel and rod strains for the first IM7/K3B 1500-hour aging	44
Figure 17. Panel and rod strains for the second IM7/K3B 1500-hour aging	45
Figure 18. Panel and rod strains for the first IM7/PETI-5 1500-hour aging	46
Figure 19. Panel and rod strains for the second IM7/PETI-5 1500-hour aging	47
Figure 20. Stress versus strain for and IM7/K3B specimen	49
Figure 21. Stress versus strain for and IM7/PETI-5 specimen	50
Figure 22. Stress versus strain for an IM7/PETI-5 specimen stressed to 85% of it's ultimate compressive stress)	51
Figure 23. Quasi-static modulus versus aging time	53
Figure 24. Quasi-static strength versus aging time	54
Figure 25. Weibull strength distribution for the IM7/K3B composite	61
Figure 26. Weibull strength distribution for the IM7/PETI-5 composite	62
Figure 27. DSC scans on IM7/PETI-5 for four aging conditions	64
Figure 28. DSC scans on IM7/K3B for four aging conditions	65
Figure 29. DSC scans on one IM7/PETI-5 sample aged for 3000 hours without compressive loading	67
Figure 30. DSC scans on one IM7/PETI-5 sample aged for 3000 hours with compressive loading	68
Figure 31. DSC scans on one IM7/K3B sample aged for 3000 hours without compressive loading	69
Figure 32. TGA for unaged IM7/K3B	71
Figure 33. TGA for unaged IM7/PETI-5	72
Figure 34. TGA weight loss rate versus temperature for unaged, aged 3000 hours with stress, and aged 3000 hours without stress IM7/K3B samples	75
Figure 35. TGA weight loss rate versus temperature for unaged, aged 3000 hours with stress, and aged 3000 hours without stress IM7/PETI-5 samples	77
Figure 36. Average derivative of weight loss rate and standard deviation for the four different aging conditions	78

I. INTRODUCTION

Today, advanced, high performance, fiber-reinforced polymer matrix composites are being considered as structural materials in supersonic aerospace applications. One such application is as a load bearing member in the High-Speed Civil Transport (HSCT) commercial airplane. A useful service life of over 60,000 flight hours is expected; and with a design cruise speed of Mach 2.4, skin temperatures of up to 177°C are expected. Because of these demanding service conditions, new experimental polymeric composites are being developed [1, 2].

A central concern with using polymer matrix composites is that the polymer properties, and therefore the composite properties, are time dependent and sensitive to aging and environmental conditions such as loading, temperature, and humidity. The long term behavior of these materials is a complicated function of many variables, including physical aging, chemical aging, thermal oxidation, damage accumulation, plastication, ect. Before using these materials in critical applications, it is important to thoroughly evaluate the various factors impacting long term durability. Various short term tests were conducted here to evaluate the materials' performance after aging under these conditions.

In this study, two carbon fiber-reinforced high-temperature polymer composite material systems, IM7/K3B and IM7/PETI-5, were thermally aged at 163°C for up to

3000 hours under compressive loading. The aged material was examined for signs of physical as well as chemical aging. Physical aging is used to explain the change in polymer properties at constant temperature, at zero stress, and under no influence from any other external conditions. Unlike physical aging, chemical aging is not thermoreversible and is sometimes referred to as chemical degradation. During chemical degradation, reduction of molecular weight can result from bond breakage and weight loss due to out-gassing of low molecular weight substances [3]. Both types of aging have been shown to have significant effects on vital material properties like strength and stiffness.

Literature Review

An in depth review of physical and chemical aging studies, past aging analysis's performed on polymeric materials, and studies done on IITRI compression testing has been conducted.

Aging

Physical and Chemical Aging

It has been well documented that amorphous materials are not in thermodynamic equilibrium at temperatures below their glass transition. The material's slow approach to equilibrium is referred to as physical aging. Physical aging occurs in materials that are at a temperature below their glass transition but above their first secondary transition or beta transition. As physical aging progresses, a material will become more glass-like, stiffer and more brittle with slower relaxation rates. An important feature of physical aging is that it is thermoreversible, which means that the prior history of an aged material can be erased by heating the material above its glass transition and requeenching [4,5].

Chemical aging, unlike physical aging, is not thermoreversible. Chemical aging or chemical degradation involves changes in material properties as well as irreversible changes in the material's structure, such as chemical modification and rupture of primary atomic bonds [3]. Oxidation, a common cause of chemical degradation, results from formation of free radicals, initiated by light, heat, trace metals, ect., and reaction of the free radicals with oxygen (O_2). The degree of degradation can be affected by the polymer structure (topology) and the amount of crystallinity (morphology). Branched polymer chains are more susceptible to degradation than linear or backbone chains since branch points have a lower dissociation energy associated with them and increased crystallinity can restrict oxygen diffusion slowing down degradation [6-8].

In a study by Parvatareddy et al. [6], the effects of elevated temperature aging on the durability of high performance polymeric composites were examined using three different aging environments; atmospheric air, reduced air pressure and nitrogen. Two carbon-fiber-reinforced resins, IM8/954-2 and IM8/ITX, aged isothermally at 150°C , were studied. In the IM8/954-2 material system, the glass transition temperature measured by Dynamic Mechanical Analysis (DMA) decreased by about thirty degrees in the first two months. In the following seven months, the T_g increased by twenty degrees. The steepest initial decline in T_g and the flattest incline was observed for the atmospheric air case. This trend implied that the largest amount of chemical degradation occurred in the material exposed to atmospheric air; and the effect of this degradation was initially greater than that of physical aging. After two months, the physical aging had a greater influence than the degradation. Similar results were seen for the IM8/ITX material; however, no initial decline in T_g was observed so the degradation never dominated in it. Results from tensile tests showed decreased strain to failure and increased modulus with increased aging time for both material systems and for all three environmental conditions. As expected, atmospheric air had the most pronounced effect while nitrogen had the least. Weight loss measurements versus aging time were also presented in this article. Again, the greatest change was seen in the atmospheric air case.

An excellent study by Bowels, Roberts and Kamvouris [9] analyzed the long term aging of carbon fiber reinforced PMR-15 composites. Five aging temperatures and specimens of different thicknesses and widths were studied for aging times in excess of 15,000 hours. Results from DMA determined that at aging temperatures below 260°C the T_g was dependent on aging temperature but not the period of aging. It was also determined that the compression strength of the material aged at temperatures above 260°C was exponentially proportional to weight loss. For the aging specimens, the thinner specimens lost their strength faster than the thicker specimens. Except for material aged at the lowest temperature, 204°C, modulus values increased slightly due to increased crosslinking during the first 4000 hr before decreasing. A difference in failure mode was seen for the different aging times. For increased aging, at a particular temperature, “brooming” failures as opposed to “wedge” failures occurred which is suggested to be the result of decreased transverse strength.

Aging in two composite systems, graphite/epoxy (A-S/3501) and graphite/polyimide (HT-S/710) was studied by Kerr and Haskins [10]. For the graphite/epoxy composite, tested in uniaxial tension at 177°C, a reduction in strength was seen after 10,000 hours of aging at 121°C. The same material aged at 177°C (tested at 177°C) showed a reduction in strength after 5,000 hours of aging. In the polyimide system (tested at 232°C) no reduction strength was seen until 50,000 hours of aging at 232°C. The same system tested and aged at 288°C showed significant losses in tensile strength after only 200 hours of aging. The primary cause of mechanical property loss was attributed to matrix degradation by oxidation.

Sell and McKenna [11] monitored the change in yield stress of epoxy-glass due to aging. During aging, the compressive yield stress of the epoxy increased. The rate of change of the yield stress with aging was initially rapid until a transition time, t^* , when it slowed significantly. The transition time shifted to longer aging times as the aging temperature decreased.

In a study by Mijovic [12], the glass transition temperature of eight-ply unidirectional graphite/epoxy composites was studied during 5,000 hours of aging. For three sub- T_g aging temperatures, relatively no change in glass transition was seen until after 1,000 hours of aging. The increase in T_g that occurred past 1,000 hours was large, up to 46°C. The proposed explanation for the result was that decreasing free volume allowed reactive groups to approach, in turn additional crosslinking caused an increase in glass transition at later aging times. To support this claim an immediate rerun of the DMA test on each aged specimen showed results almost identical to the specimens first run indicating irreversible chemical aging.

The effects of crosslink density on physical aging was examined by Lee and McKenna [13]. For an epoxy network, it was observed that the shift rate for the stress relaxation time-temperature superposition decreased with increasing crosslink density. In a study by Sullivan, Blais, and Houston [14] physical aging was seen in polymer systems with varying amounts of crystallinity. The materials studied were thermosetting and thermoplastic composites and their separate polymer matrices. Good time-temperature superposition was observed for the amorphous material but the semi-crystalline polymers exhibited strong aging effects at temperatures above T_g . This “extended glass transition” was explained in detail by Struik [15].

Physical aging has been found to be dependent on gas absorption. As a material ages free volume decreases so inert gas solubility decreases. Conversely, gas absorption occupies free volume which slows physical aging [16]. Aging has also been discovered to affect impact toughness. Chen-Chi et al. [17], showed for poly(ether ether ketone) (PEEK) and poly(phenylene sulfide) (PPS) that damage initiation forces decrease after forty-eight hours of aging. Damage initiation force also decreased with increased aging temperature.

Viscoelastic creep, or deformation accumulation over time, in polymers occurs because of chain mobility which is dependent on free volume and configurational entropy. As a polymer ages it's configurational entropy and free volume decrease which decreases

chain mobility and increases structural relaxation time [16]. Sullivan, Blais, and Houston [14] observed decreasing compliance and decreasing log rate of change of compliance with aging for several glass fiber reinforced resins. Gates and Feldman [18] performed a sequence of isothermal creep and recovery tests on IM7/8320, thermoplastic composites, to produce master curves. They discovered that for temperatures close to T_g superposition does not accurately predict strain recovery [15,18].

Sullivan [19] showed that the tensile creep compliance of composites, in the fiber direction, is virtually independent of aging effects. It was also discovered that time-temperature superposition (TTSP) is only applicable to momentary creep in composites. Using TTSP for longer aging times resulted in large over-estimates. A model describing the creep deformation of poly(buthlene terephthalate) (PBT) was created by Dean, Read and Tomlins [20]. To evaluate the parameters in the model, long term data was needed since extrapolations from short term tests were not accurate enough. The model worked well for PBT however, no other materials were analyzed.

Peng [21] solved a set of equations, derived in an earlier paper, describing the relaxation behavior of time dependent chemically unstable materials for specific loading conditions. One particular loading condition examined was stress relaxation under constant strain. The result was an equation for change in modulus over time with constant temperature. Another paper by Seitz [22] used empirical and semi-empirical relationships to estimate mechanical properties of polymeric materials. Equations were derived for modulus, Poisson's ratio and tensile yield stress in terms of molecular weight, van der Waals volume, the length and number of rotational bonds in the repeat unit, and the T_g of the polymer.

DSC and TGA

In a review by Hutchinson [3] of the physical aging of polymers, the fundamental techniques behind DSC were explained. One important trend that he described was that as

the aging time of a polymer increases, typically the magnitude of a glass transition peak, in a specific heat versus temperature plot, increases and shifts to higher temperature [3,23]. Berens and Hodge [24] displayed experimental evidence of this T_g “overshoot” for PVC. The dependence of this phenomenon on varying pretreatments was demonstrated with numerous experimental tests. In a follow up paper on the same topic, Berens and Hodge [25] used a four parameter mathematical model to reproduce DSC data for PVC and other polymers.

The ability to predict the mechanical behavior of aging materials from DSC results would be very useful. This idea would not only save material and time expended on specimen preparation for mechanical tests, but it would replace long term aging studies with short term tests. In order for this to happen, the relationship between the two different time scales, DSC and mechanical, needs to be determined. Echeverria et al. [26] used a reduction procedure (described in the article) and data from DSC tests, performed on a polyetherimide material aged for up to 192 hours at various aging temperatures, to produce a master curve. This master curve is the first step in determining the relation between DSC results and mechanical aging results. Next, the effects of long term aging on mechanical properties need to be correlated with the DSC results.

Thermogravimetric analysis (TGA) has been widely used to study the thermal decomposition of polymers. Dynamic TGA allows weight loss rate versus temperature to be monitored. From this weight loss rate versus temperature data, an Arrhenius activation energy can be calculated and used to extrapolate weight loss results to lower temperatures and longer times. Also, differences in weight loss rate versus temperature curves are known to be representative of differences in degradation mechanisms [27]. Cunningham [28] devised a two reaction model to quantitatively describe the different degradation mechanisms present in his TGA results. His model assumed that the degradation behavior consisted of bulk thermal mechanisms occurring within the material and diffusion dependent oxidative mechanisms occurring near the material surface. Experimental tests on PMR-15 powder showed good correlation with the model.

A study by Lin and Pearce [29] analyzed the effects of aging on an epoxy, diglycidyl ether of bisphenol A (DGEBA) cured with trimethoxyboroxine (TMB). As expected, the weight decreased with aging and the rate of weight loss increased with increased temperature. To explain the weight loss, an equation for diffusion of volatile products, in terms of kinetic parameters, through the solid was derived assuming that that diffusion step was rate determining. The theoretical results agreed with the experimental results therefore confirming the assumption made previously. It was also mentioned that vacuum TGA allows the rate-controlling step to be shifted from a diffusion process to a chemical process. Using this method, kinetic parameters for a non-reversible reaction could be determined.

Only one report was found that examined the combined effects of aging and loading. Lahrman et al. [30] studied the effects of compressive loading combined with 1500 hours of aging on IM7/K3B (graphite/epoxy) sixteen-ply quasi-isotropic composites. Two aging temperatures, 250°F and 350°F, produced statistically different residual strength values; however, only the residual strength of the material aged at 350°F (in the Battelle fixture) showed decreased residual strength with aging time. There were no significant trends observed in the modulus values throughout the aging.

Compression Tests

A comparison between shear loaded compression and end loaded compression was performed by Berg and Adams [31]. Two shear-loaded coupon test fixtures, the Illinois Institute of Technology Research Institute (IITRI) fixture and the modified Celanese fixture, and one end-loaded coupon test fixture, the Wyoming end-loaded side-supported fixture, were compared. Tabbed unidirectional $[0^\circ]$ and quasi-isotropic $[+45^\circ/0^\circ/-45^\circ/90^\circ]$ carbon/epoxy specimens were examined using the three fixtures. Results of the compression tests showed that for the unidirectional material, modulus values were not

statistically comparable between the shear loaded and end loaded fixtures. Despite large scatter in the ultimate compressive strength results, all three fixtures produced statistically similar results for the unidirectional specimens. For the quasi-isotropic specimens, all three test fixtures showed similar results, with the IITRI fixture producing slightly higher ultimate strength values and lower experimental scatter in the moduli values.

A similar study by Poon [32] reported that end loading was satisfactory for carbon/epoxy quasi-isotropic fabric composites which produced failure by fiber kinking. However, end-loading was found to be unsatisfactory in unidirectional $[0^\circ]$ fiber-reinforced specimens which produced longitudinal splitting and premature failure. Whitney and Guihard [33] compared compression results obtained from the standard IITRI fixture with results from the mini-sandwich beam. The mini-sandwich beam attempts to replace the complex failure mode associated with IITRI with fiber failure only. Results of the compression tests on graphite/epoxy composites, with various lay-ups, including unidirectional, showed higher ultimate compressive stresses when using the mini-sandwich beam. This result was attributed to the difference in failure modes; fiber failure using the min-sandwich beam versus delamination using the IITRI fixture.

In compression analysis it is assumed that a uniform stress state exists in the test section. Daniels and Sandhu [34] used finite element analysis to compare gage section stress states between IITRI and several other compression fixtures with varying tabbing geometry's. Results showed that the IITRI fixture produced high stress concentrations in the region of the end tab. The most uniform stress state with the highest average compressive failure load was found using the Rolfes fixture, a shear loaded fixture similar to IITRI, with a Sendeckyj-Rolfes specimen.

The effects of different tabbing material on compression strength was studied in more depth by Odom and Adams [35]. Steel and glass/epoxy tabbing materials, in addition to a wide variety of tabbing geometry's: tapered, un-tapered, un-tapered partial grip and debonded were examined. IITRI compression was performed on unidirectional carbon/epoxy specimens possessing various combinations of tabbing materials and

geometry's. The results indicated that failure mode was strongly influenced by tabbing material and geometry. Un-tapered glass/epoxy tabs produced relatively high compressive strengths if not the highest.

Summary

The aging studies reviewed attempt to quantify the effects of physical and chemical aging on polymeric composites. The effects of different aging temperatures, aging environments, aging times and specimen dimensions, ect. on glass transition temperature, strength, and stiffness were documented for a variety of material systems. Kerr and Haskins' study and several other long term studies demonstrated that for continuous carbon fiber composites, the effects of physical and chemical aging on mechanical properties can be substantial even for sub- T_g aging temperatures and aging times of less than 10,000 hours. The progress of high-temperature polymer matrix composites so far is promising, but prior to the commercial use of these materials in high-temperature aerospace applications, studies involving aging times of the order of the lifetime of a commercial aircraft (60,000 hours) need to be examined.

From the thermogravimetric studies done, it was found that different degradation mechanisms can be observed in weight loss rate versus temperature curves. In a preliminary report, one author attempted to model these degradation mechanisms. A quantitative description of how these degradation mechanisms change with aging time could prove to be useful. The changes in degradation with aging would verify that a modification due to chemical aging had occurred in the material. The majority of the aging studies examined in this review only qualitatively described any polymer degradation and it's relevance to mechanical properties changes over time.

Problem Statement

For some time now physical aging, the slow and gradual approach to equilibrium of a solidified supercooled liquid [4], has been a concern when studying polymer matrix composites. Long term aging, of materials used in the HSCT, at elevated temperatures could cause chemical in addition to physical aging. Unlike physical aging, chemical aging is not thermoreversible. This chemical aging or degradation often involves molecular weight reduction, due to scission of chemical bonds, and loss of lower molecular weight substances through out-gassing. As reported in the literature review, the combination of physical and chemical aging can have drastic effects on material performance. Therefore, due to the expected demanding service environment of the HSCT, studies of polymeric materials being considered for use need to analyze long-term physical as well as chemical aging.

In addition to monitoring the effects of physical and chemical aging, this study is one of the first to incorporate the combined effects of loading and aging. This study examined the effects of sub- T_g aging on two high performance polymeric composite systems under static compressive loading. The Illinois Institute of Technology Research Institute (IITRI) compression test method was used to evaluate changes in modulus, strength, and failure strain over 3000 hours of aging. Weibull statistics were used to evaluate changes in scatter of the residual strength data. Changes in T_g were monitored using DSC. Dynamic TGA tests were used to find the weight loss rate versus temperature results for the different age materials and compare any changes in their degradation mechanisms. In summary, this effort analyzed the effects of physical aging and chemical aging through the use of compression testing, DSC, and TGA.

II. EXPERIMENTAL PROCEDURES

Material

The two carbon fiber-reinforced polyimide material systems examined in this study were IM7/K3B and IM7/PETI-5. Both composites had a quasi-isotropic lay-up, $[+45/-45/0/90]_{2S}$ for IM7/K3B and $[+45/0/-45/90]_{2S}$ for IM7/PETI-5, with a fiber volume fraction of 60%. The IM7 fiber is an intermediate-modulus carbon fiber previously surface-treated and sized (Hercules Product Data sheet) [36]. The K3B matrix material, a DuPont product, is a high temperature thermoplastic polyimide with an unaged glass transition temperature of 237°C as determined by DSC [37]. The autoclave processing temperature of the IM7/K3B composite was 650°F (343°C). The PETI-5 matrix material is a phenylethynyl terminated imide oligomer. Both PETI-5 and Boeing/DuPont's K3 polymers were designed to have enhanced processability and better high-temperature stability. For PETI-5 a range of glass transition temperatures 210-262°C is given by Hergenrother and Smith [38] for various molecular weights and concentrations of main constituents. The 16-ply composite materials used in this study were furnished by The Boeing Company in pre-cut 76.2 mm by 139.7 mm panels. The IM7/K3B panels were cut

from one parent panel processed at Boeing. The IM7/PETI-5 coupons were cut from two parent panels cured as a single batch by Nothrop-Grumman Corporation in Hawthorne, CA, from prepreg furnished by NASA-Langley Research Center. Twenty-four out of thirty-seven original 76.2 mm by 139.7 mm panels (12 IM7/K3B and 12 IM7/PETI-5) were selected for aging while the rest were used for baseline comparisons and thermal compensation.

Environmental Conditioning

The Boeing Company provided twenty compression fixtures designed to apply strain to the aging panels. The stainless steel fixtures consisted of two 25.4 mm thick square plates, four threaded reaction rods (Custom 450 stainless steel), and a pair of anti-buckling restraints. The fixtures were designed to compressively strain a panel inserted between the two steel plates by tightening nuts on the four reaction rods Figure 1. The buckling restraints prevented buckling of the loaded panel while it was being strained at room temperature. The strained panel-fixture assembly was then placed in either a precision Fisher Scientific convection oven or a Blue M programmable convection oven for aging at 163°C.

In order to monitor the initially applied panel strain and changes in that strain during aging, two high temperature WK-125AD-350 gages were adhered to each panel. One strain gage was centered on each 76.2 mm by 139.7 mm side of the panel. This strain gage configuration is referred to as back-to-back later in the text. All strain gages and gaging accessories were acquired from Measurements Group unless otherwise noted. A 25.4 mm by 76.2 mm temperature compensation specimen was also gaged for each material system. Temperature compensation was used in a half-bridge configuration to subtract out the effects of temperature and aging. The WK-gages and their bondable terminals were applied to each panel by first lightly sanding the gage area with 600-grit silicone-carbide paper and then adhering each gage with M-Bond 600 adhesive. In order

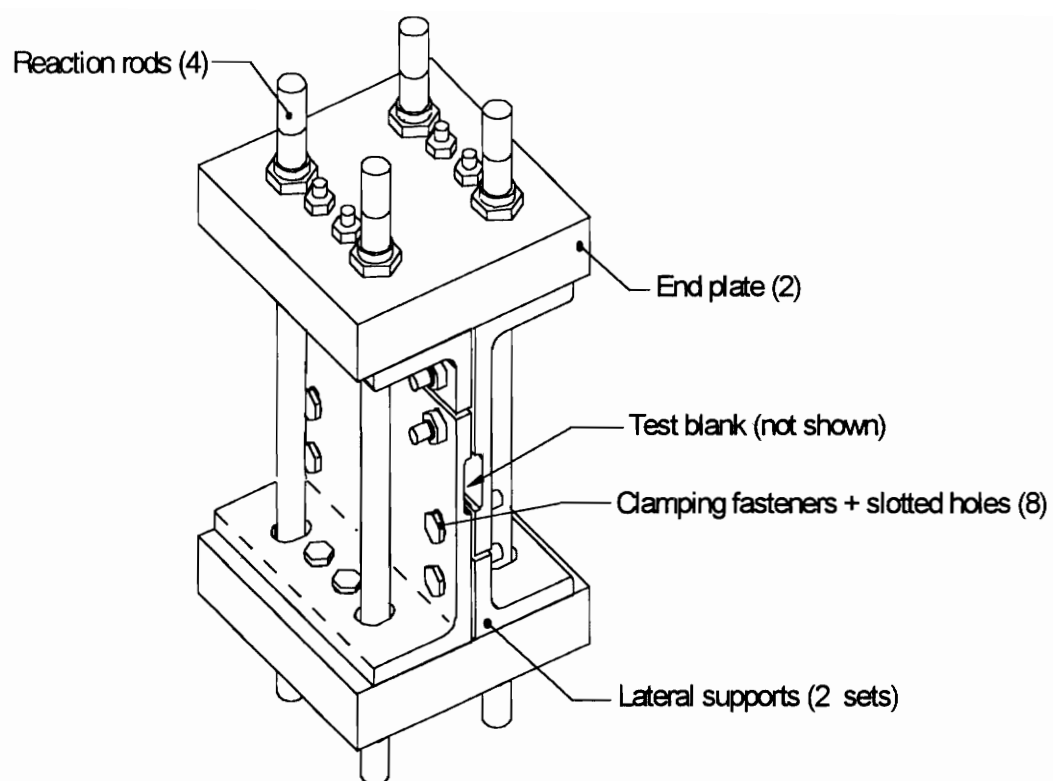


Figure 1 Loading fixture (Drawing courtesy of Boeing).

to cure the adhesive, a 100 N force was applied to panel and gages using a spring clamp. The clamped panel and gages were heated at a rate of 11°C/min and then held at 120°C in a Fisher Scientific programmable convection oven for two hours. The adhesive was post-cured at 205°C for one hour and fifty minutes with the spring clamp removed. WK-gages were also used to monitor strain in two of the four reaction rods, on one diagonal, of each fixture. Prior to gaging the reaction rods, each rod was sanded and then cleaned with M-Prep Conditioner A and M-Prep Neutralizer 5A. The WK strain gages were then applied to the rods in a manner similar to the panels.

The pre-attached strain gage lead-wires and Teflon coated external wires (430-FST, four-conductor cable) were soldered onto the two terminals bonded below the gages with high temperature solder, 430-20S-25. An additional layer of M-Bond 600 adhesive was applied covering the entire strain gage and solder connection to protect them from the thermal aging environment. The adhesive layer was subsequently cured at 120°C for two hours. All lead wires from the strain-gages were directed through special openings in aging ovens so that strain measurements could be taken without opening the oven door. In order to monitor panel temperature more accurately, each panel had a separate thermocouple attached to it. The thermocouple wires were fed through the same openings as were the strain-gage lead wires.

For convenience, the panels were strained at ambient temperature. The procedure was as follows. First, the strain-gages were balanced and calibrated with the panel resting between the lateral buckling restraints on the base plate of the fixture. Second, the top plate was placed on the assembly and allowed to rest on top of the panel. Bolts on the buckling restraints were only finger tightened which allowed movement due to thermal expansion. The strain gages and the wiring were protected by an undercut in the lateral buckling restraints (Figure 2). Third, the nuts on the reaction rods were tightened. The nuts were tightened one at a time by approximately an eighth of a turn at a time. In order to keep the fixture steady, without having to clamp it down, the fixture was rested on top of a vice (Figure 3). The nuts were tightened in a criss-cross manner which means that after

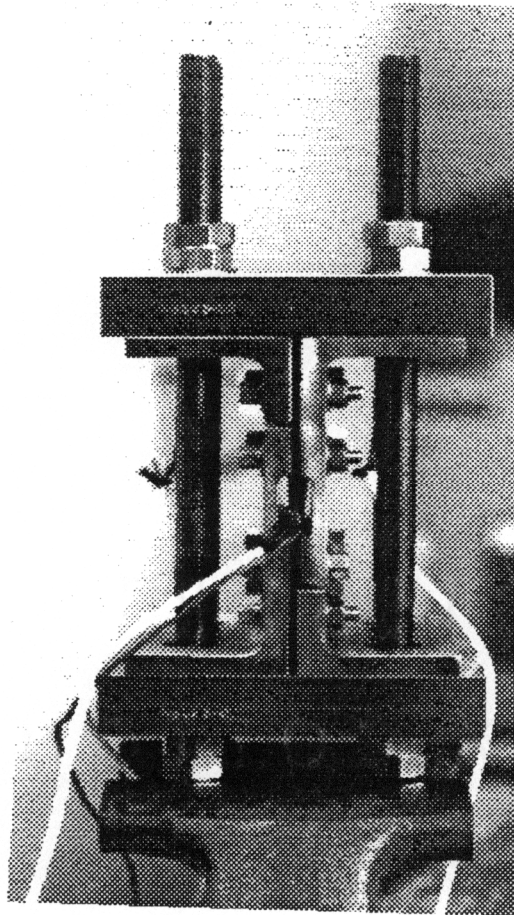


Figure 2 Loading fixture (panel edge view).

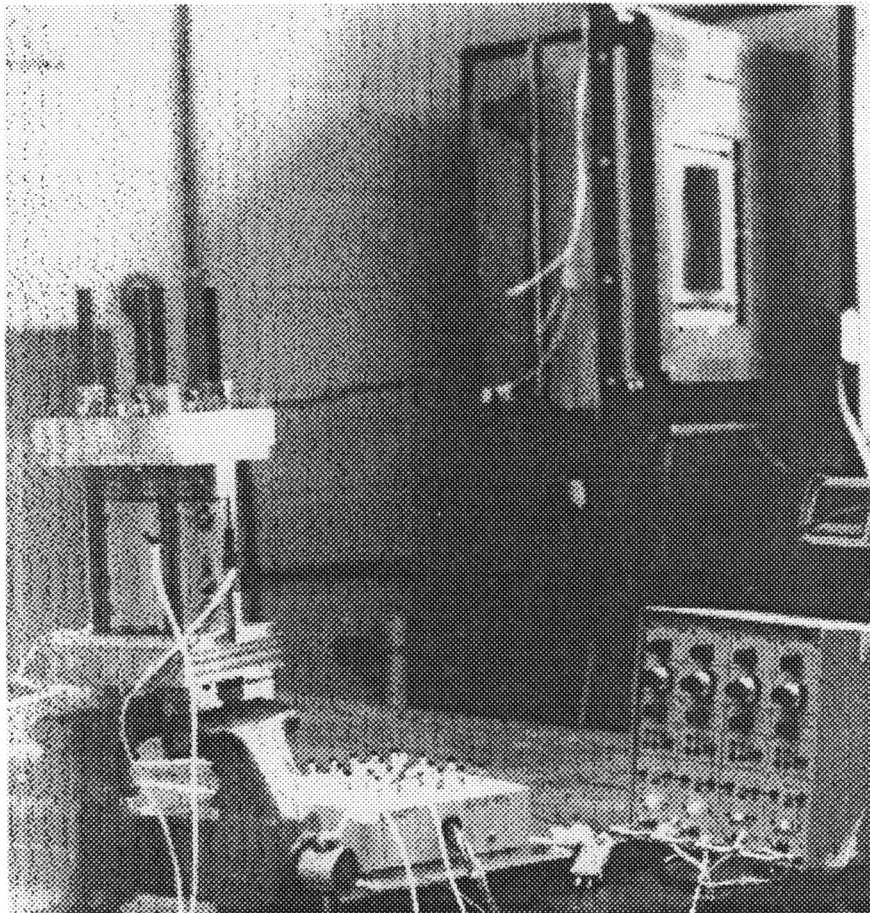


Figure 3 Straining and aging setup for the panel-fixture assembly.

one nut was tightened the nut on that same diagonal but on the opposite side of the panel was tightened. This was then repeated for the other diagonal. The percent bending was kept below 10% during the straining. Fourth, when the measurements from the gages on the panel reached the desired level, the straining was stopped. Fifth, as each panel-fixture assembly was finished, it was placed in the oven at room temperature.

When a negatively pre-strained panel is put into a heated oven, the magnitude of the strain will decrease due to thermal expansion of the fixture and the panel. The panel strain reduction was estimated with a simple 1-D model (Appendix A) and the amount of pre-strain required at room temperature was calculated given the modulus, coefficient of thermal expansion, and cross-sectional area of the panel and reaction rod. Several iterations were performed to acquire 2000 ± 100 micro-strain for all of the panel-fixture assemblies: heating the assemblies to 163°C , checking the strain level, cooling to room temperature, and adjusting the strain level.

For this study, panels were aged at 163°C for 1500 and 3000 hours. Eight panels for the 3000-hour aging were placed in the Blue M oven along with eight 10,000-hour panels which were not tested in this study (Figure 4). The eight 1500-hour panels were aged four at a time in the Fisher Scientific oven. Placed in each oven was a temperature compensating steel rod and two temperature compensating composite panels one for each material system. After the first 1500-hour aging, the four aged panels were replaced with four unaged panels; but the same temperature compensation panels were used for the first and second 1500-hour aging segments.

In order to monitor changes in stiffness or strain in the thermal aging test fixture, panel and reaction rod strains were recorded every 250 hours. Prior to straining each panel, a half-bridge strain gage circuit was balanced and calibrated with two match-pair precision resistors (H2-350-01) in the external half-bridge. The precision resistors were then replaced by an “active” gage on the specimen to be compressively loaded and a “dummy” gage on the temperature compensation specimen. The resultant voltage output from the bridge circuit was the reference for that particular active gage in combination

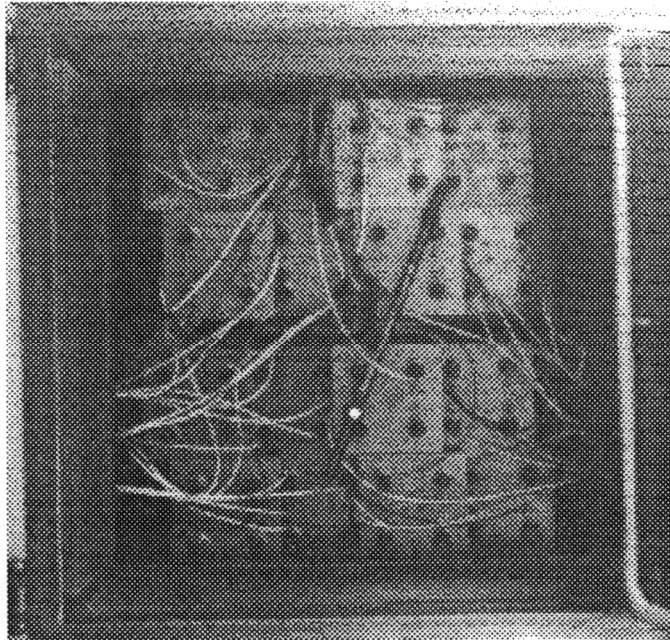


Figure 4 Blue M aging oven containing the sixteen aging fixtures.

with that particular dummy gage. This procedure was repeated prior to straining each panel. Before strain readings were recorded during the aging, the half-bridge circuit was balanced and calibrated with the same matched-pair resistors used to obtain the reference. The resistors were then replaced with the active gage and dummy gage and the resultant voltage output minus the reference was the actual strain. For all strain readings, the same 2200 amplifiers and half-bridge completion box were used.

Specimen Preparation

Compression Tests

For the IITRI compression tests, untapered glass/epoxy tabs were adhered to each 76 mm by 139 mm panel to reduce stress concentrations induced from gripping the specimen. The tabbing material and tab geometry was chosen based on the work of Odom et al. [35]. The adhesive used was a two part epoxy adhesive (DP-420), manufactured by 3M, which cured in two hours at 50°C. Care was taken to ensure in-plane alignment of the fiber direction to the tabs and hence the loading of the specimen. This was made possible by a 152 mm by 152 mm tabbing fixture which allows the application of tabs to one side of a panel relative to a reference for the fiber direction (Figure 5). To produce a uniform bond thickness, several pieces of 0.178 mm diameter wire placed between the tabbing material and the composite.

Prior to applying the tabs, both sides of each panel were lightly sanded with wet 400 and 600-grit silicone-carbide paper to increase the bonding surface area. The tabs were also roughened by sand-blasting on one side. A 13 mm Teflon spacer was used to create the desired gage length, and its beveled edges allowed adhesive spew to cure at an angle of 45° with the specimens surface (Figure 6). This prevented the formation of a singular stress field at the bi-material interface. With tabs adhered to one side of the panel, the thickness of the tabs was ground flat and parallel to the plane of the panel. Tabs were

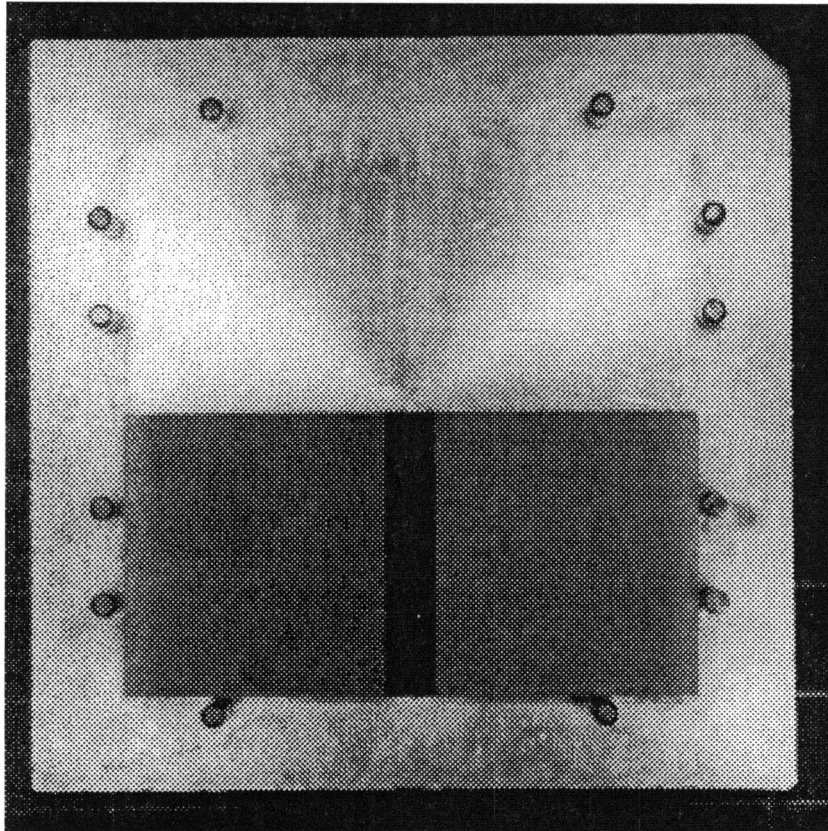


Figure 5 Tabbing fixture and tabbed composite panel.

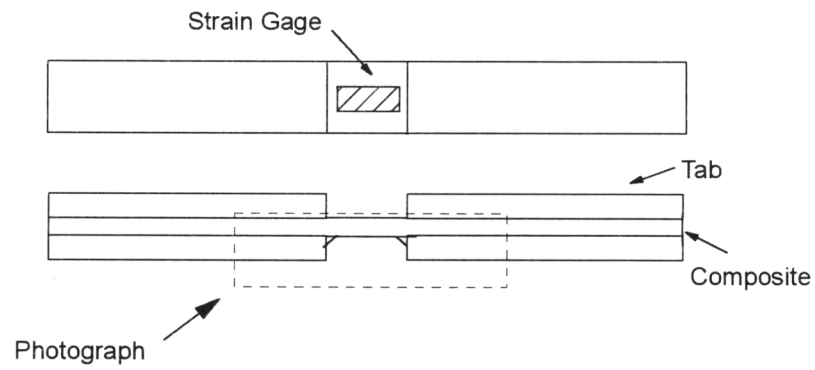


Figure 6 Specimen sketch (a) top view (b) edge view and lose-up photograph of a tabbed specimen (edge view) displaying a typical spew angle.

subsequently applied to the opposite side. These tabs were then ground to make them flat, parallel, and of equal thickness to the tabs of the opposing side. This ensured that the out of plane alignment of the panel was true to the loading axis. One attempt was made to tab two panels at once, since each panel width was 76 mm and the tabbing fixture was 152 mm wide, but the resulting tabbed composites came out slightly warped requiring extra grinding.

Specimens were cut with a water cooled, diamond-tip blade; and then the edges were ground to a nominal width of 12 mm. For the aged samples, a buffer of 5.1 mm was cut from the edges of the original 76 mm wide panel so that only uniformly aged material was tested. The finished specimens were lightly wet-sanded with 600-grit silicone-carbide paper and then instrumented with back-to-back CEA-06-250UN-350 strain gages. Room temperature curing M-Bond 200 was used to adhere the strain gages. All of the prepared samples were dried in a vacuum at 60°C for twenty-four hours and then stored in an active desiccator until being tested. On the day of testing, approximately ten specimens at a time were wired with twisted four conductor cable (426-DTV) and 361A-20R solder (Figure 7).

DSC and TGA

For the DSC and TGA experiments, very little specimen preparation was required. Thin strips, 2.54 mm wide, of composite were cut and then small pieces (approximately 15 mg.) were cut from the thin strip as needed. For the DSC tests, the 15 mg. of composite were sealed in an aluminum pan prior to testing. For the TGA tests, two pieces of composite (approximately 40 mg. total) were placed in an open platinum pan prior to testing.

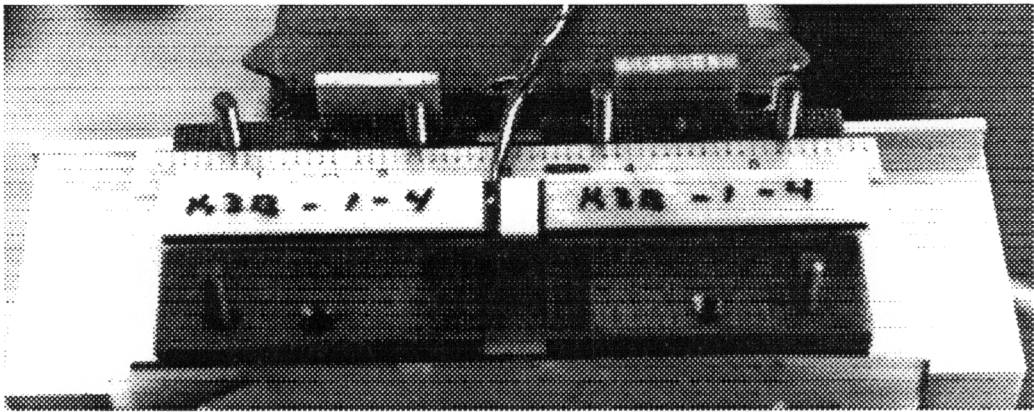


Figure 7 Wired IITRI specimen aligned in the grips.

Mechanical Tests

IITRI Compression

IITRI quasi-static compression tests were performed with glass/epoxy tabs under the guidance of ASTM D3410-94 procedure B [39]. A specimen alignment jig was used to ensure that the specimen was centered in the grips and aligned with the loading direction (Figures 7). After the specimen was secured but still in the alignment jig, the strain on the back-to-back CEA-gages was zeroed. The specimen, secured in the grips, was then placed in the IITRI fixture (Figures 8-9). Room temperature displacement controlled tests were performed using a displacement rate of 1 mm/min on a 150 kN screw driven Instron machine. This translates to a strain rate of 0.0787 mm/mm/min.

A 150 kN load cell was used to monitor the applied load while the back-to-back strain gages measured compressive strain and degree of out of plane bending. Prior to beginning every test, the specimen being tested was loaded to 400 Newtons in order to seat the fixture grips. A quarter-bridge configuration with 2300 amplifiers was used to read the strain signal while a LabView data acquisition program (written by Bob Simonds) was used to record and store the load-strain data. The stored data was input into a spreadsheet where conversion from volts to strain and stress was performed. A data regression was done on the linear portion of the resulting stress-strain relationship (0.001 mm/mm to 0.005 mm/mm) to determine modulus. The average out of plane bending in this region was usually under ten percent which was acceptable according to ASTM D3410 [39].

Differential Scanning Calorimetry

To monitor changes in glass transition temperature, DSC was performed on a DuPont 910 differential scanning calorimeter. ITCA standard method was used with a

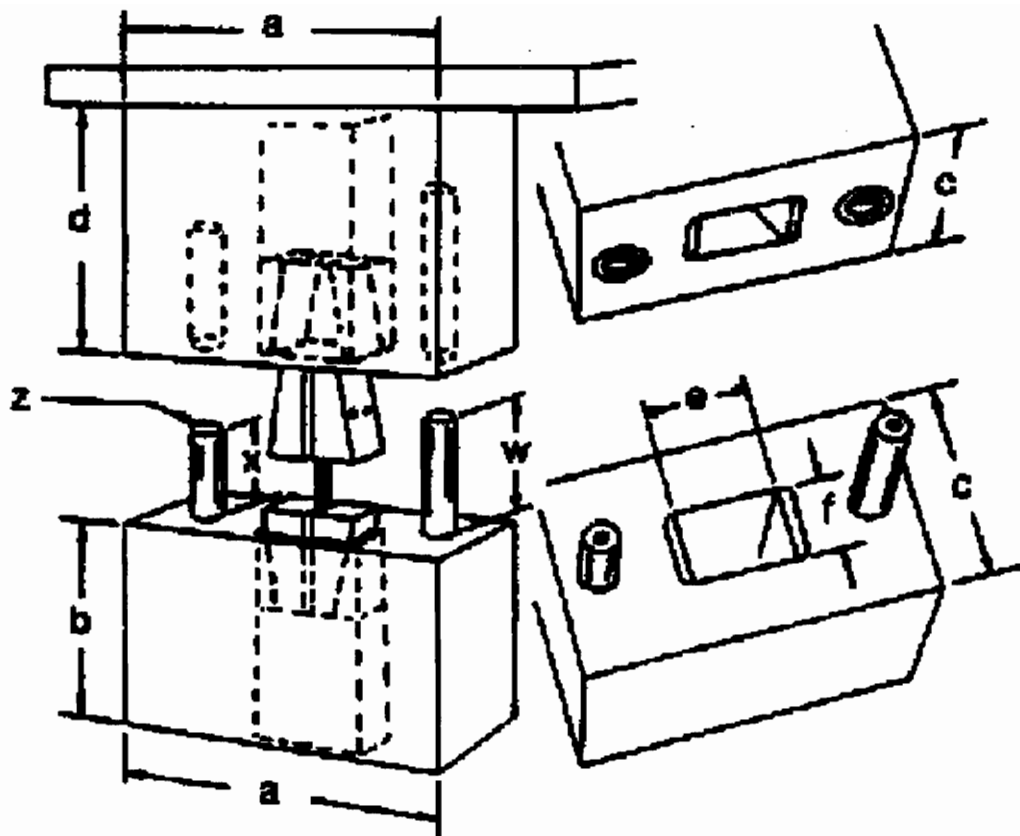


Figure 8 ITRI compression fixture diagram (ASTM).

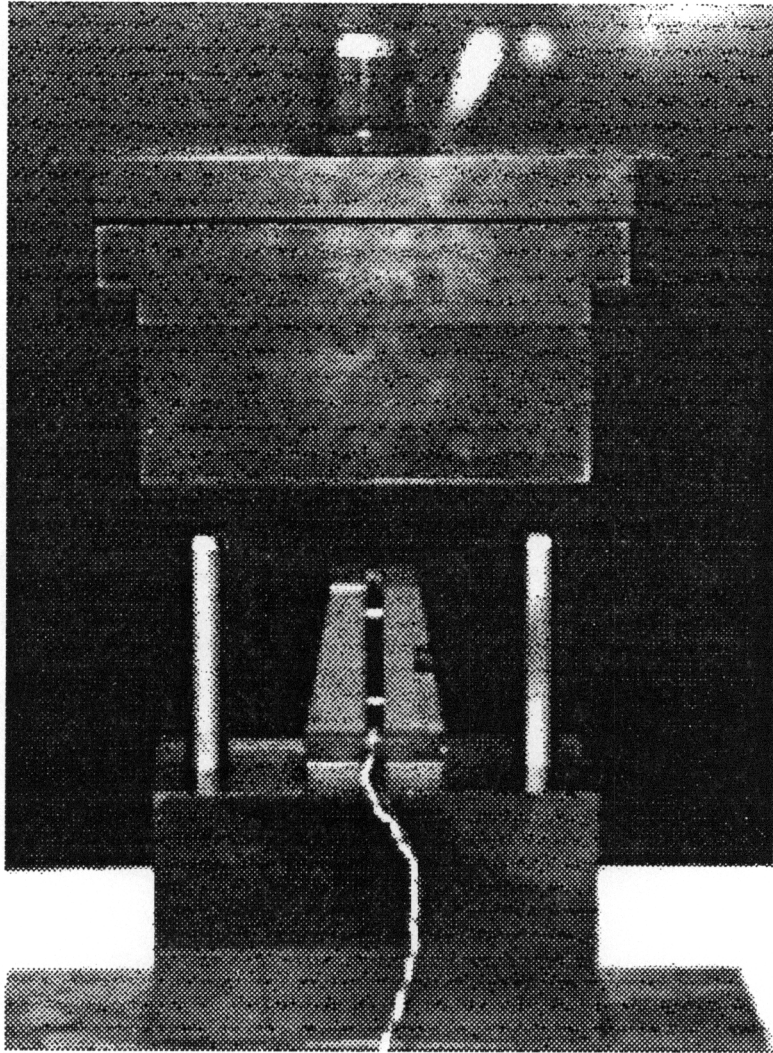


Figure 9 IITRI compression fixture and gripped specimen.

heating rate of 10°C/min to heat the sample from 150°C to 350°C. A nitrogen flow rate of 15 cc./min was used to remove any water in the system or any volatiles given off during the test. After heating, the sample was cooled using water and then reheated to 350°C with the same heating rate. Three heat-quench runs were performed on the samples from each material system to make sure that the samples were not degrading during the heating. The second and third run at each aging time was compared to the second and third run of the corresponding baseline material to see if the material had been fully rejuvenated or if chemical aging had occurred. Each day prior to testing, a new background was recorded by running a test on an empty reference pan. This background was then subtracted from the acquired data before any analysis was performed.

Thermogravimetric Analysis

TGA was performed on a DuPont 951 thermogravimetric analyzer. Using a heating rate of 10°C/min, a baseline sample, a sample aged for 3000 hours, and a sample aged for 3000 hours under compressive loading, from each material system, was burned in an air and nitrogen environment. The air and nitrogen flow rate used was 40 cc./min. From these tests, weight loss rate versus temperature data was acquired. This data was then used to model degradation mechanisms occurring in the composites.

III. EXPERIMENTAL RESULTS AND DISCUSSION

Applied Aging Strain

3000-Hour Panels

The fixtures used in this study were designed to apply a compressive load to the aging composite panels. The viscoelastic properties of the composites and the panel-fixture assembly equilibrium requirements create a mixed state of creep and stress relaxation. Due to this mixed state, the panel strain change over time is difficult to predict. The average strain from the back-to-back panel gages and the average change in the rod strain versus time for the panel-fixture assemblies aged for 3000 hours is displayed in Figures 10 and 11. The error bars represent the range of the average back-to-back panel strains for the eight panels of a particular material system. The change in rod strain was used to represent the data because the magnitude of the rod strain was small due to the high stiffness of the steel. Any error in the rod offset measurement caused a substantial error in the measured rod strain. This error would shift the measured rod strain but would not affect the change in rod strain over time.

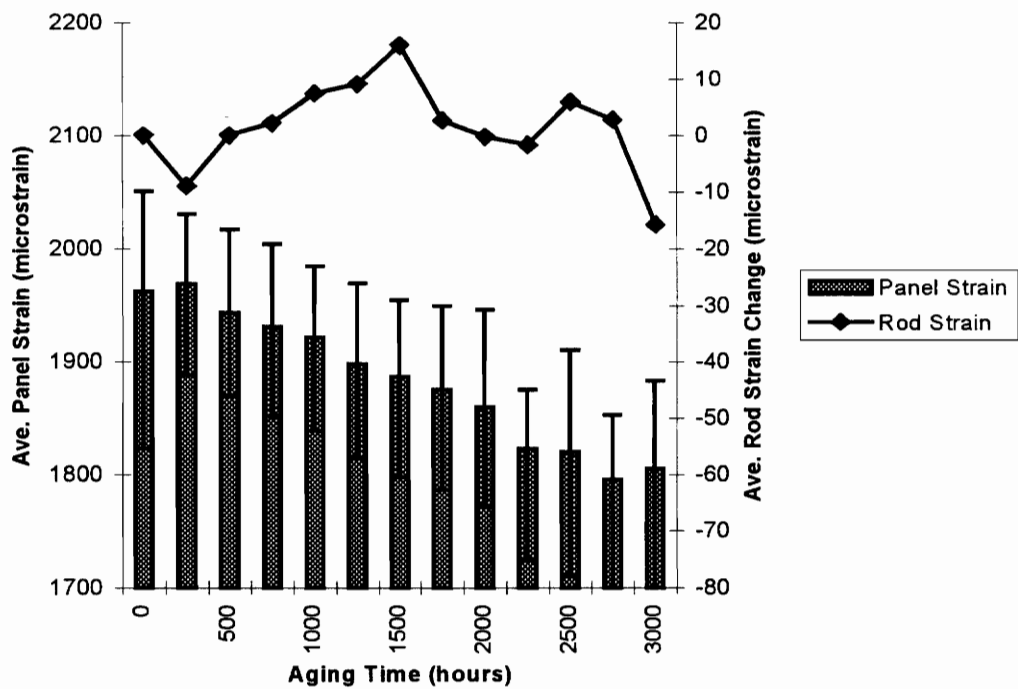


Figure 10 Average panel and rod strains for the IM7/K3B material aged for 3000 hours.

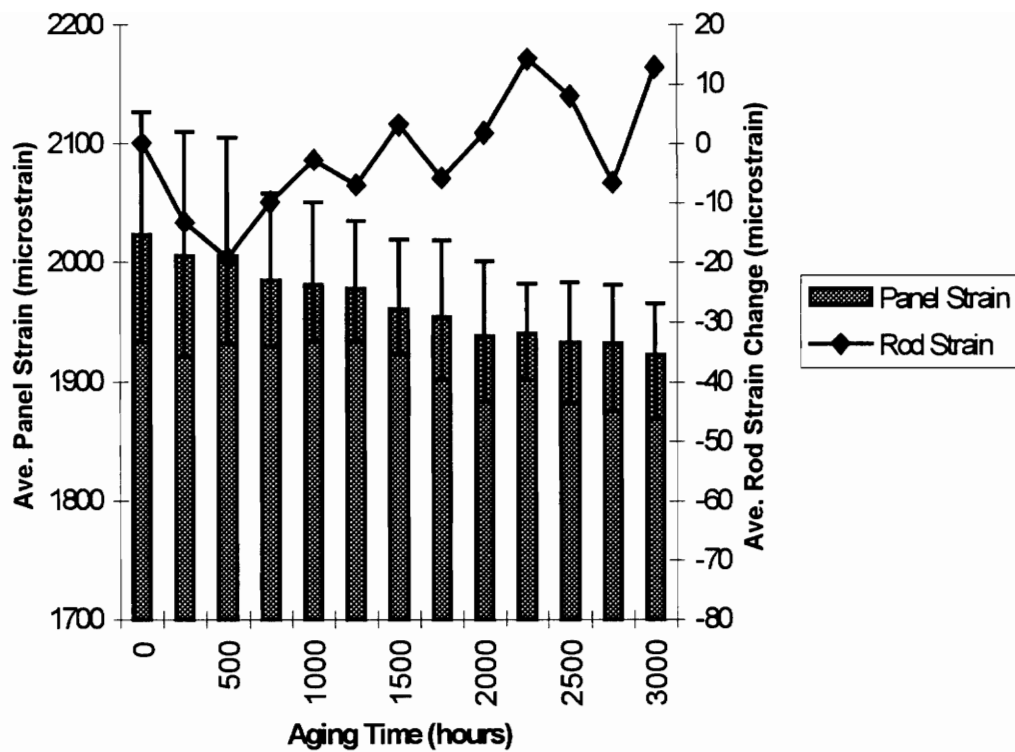


Figure 11 Average panel and rod strains for the IM7/PETI-5 material aged for 3000 hours.

It is clearly seen that the panel strains were not constant throughout the aging. While this decline in panel strain was small, less than 10%, explanations for the decline were pursued in order to satisfy a strict 5% tolerance on panel strain required for this project. The rod strains appear to have remained fairly constant. Again, due to the high stiffness of the steel, the magnitude of the change in rod strain is about one-tenth that of the panels which approaches the sensitivity limit of the gages. It is also evident from the plotted data that the rate of strain change in the panels differed between the two material systems. As seen in Table 1, the slope of the 3000-hour IM7/K3B strain decline ($0.061 \mu\epsilon/\text{hour}$) was almost double that of IM7/PETI-5 ($0.033 \mu\epsilon/\text{hour}$).

It is not clear if this was the true strain in the panels or an artifact of this method of monitoring strain. After considering possible explanations for the decrease in panel strain, it was concluded that the actual panel strain was not being reflected by the strain gages. The following explanation describes the reasoning behind this conclusion. Several possible causes for the decline in panel strain were explored in order to prove that the strain measured was not the actual strain in the panels. Assuming that the nuts on the reaction rods did not move and that the buckling restraints did not hinder the expansion or contraction of the aging panels between the end plates, then the actual compressive strain in the panels could not decrease without one of the following: an application of an external force, a progressive increase in the composite coefficient of thermal expansion, a steady increase in oven temperature, a large increase in composite modulus (due to physical aging), or some combination of the above.

The conclusion that the strain readings did not reflect the actual panel strain is clearly seen by considering the scenarios of stress relaxation and creep. For example, assuming a pure stress relaxation condition (constant strain), as stress in the panel decreases so will the apparent modulus of the panel. However, in order to maintain equilibrium in the fixture, the load in the four reaction rods must decrease proportionally to load in the panel. This decrease in rod load (or stress) implies a decrease in rod strain (Hooke's Law). Finally, the decrease in rod strain brings the end plates closer together

Table 1 Slope of the strain decline in the compessed panels with aging time.

Aging Time (Hours)	PETI-5 Regression Slope ($\mu\epsilon$/Hour)	K3B Regression Slope ($\mu\epsilon$/Hour)
3000	0.0328	0.0610
1500A	0.0011	0.0567
1500B	0.0949	0.0312

increasing the compressive strain in the panel. Similarly, for the case of creep or some combination of creep and stress relaxation, a progressive increase in compressive strain would result.

If the quasi-static modulus of the panel increased due to physical aging, more than the apparent modulus decreased, then the panel strain could theoretically decrease. No change in the room-temperature quasi-static modulus was seen over the 3000 hours of stressed aging (discussed in the next section). Frictional forces acting on the fixtures would restrict their thermal expansion which would increase the compressive strain observed in the panel. However, the frictional forces are small in comparison to the thermal expansion forces; and this would not explain the decrease in panel strain over time. The composite's CTEs, measured experimentally, were unchanged throughout the aging. The temperature of each panel, recorded every 250 hours, remained constant to within 1°C over the 3000 hour aging period. From these facts, it appears that the measured strain could not have been the actual strain in the aging panels.

If the strain measured was not the actual strain in the panels, then three possible explanations for the decline in panel strain include the following: creep of the adhesive between the strain gage and the panel, corrosion of the gage, and a difference between the physical or chemical aging rates of the compensation panels and the loaded panels. In support of this, the effects of strain gage adhesive creep and corrosion of the gage foil have been documented by Shay [40]. Shay examined strain gage stability of several high temperature gages (similar to the WK-gages used in this study) adhered to stainless steel beams statically loaded in tension and compression over a three year period. The aging temperature used was 150°C, and the applied strains were $\pm 780 \mu\epsilon$ and $\pm 1350 \mu\epsilon$.

Shay's results show an increase in the measured tensile strain and a decrease in the measured compressive strain over time (Figures 12-13). Several unloaded specimens were also examined which showed an increase in the measured tensile strain over time (Figure 14). The strain change over time decreased with increased strain gage width. The suggested cause of the strain change was the combined effect of strain gage adhesive

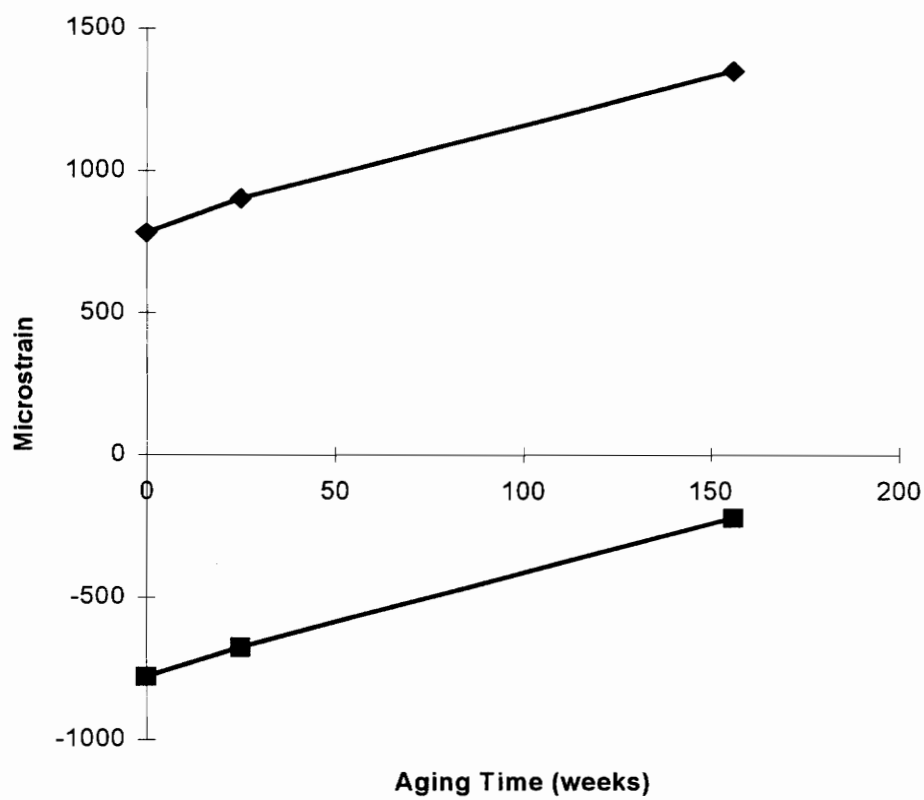


Figure 12 Three year strain history for initially applied strains of $\pm 780\mu\epsilon$.

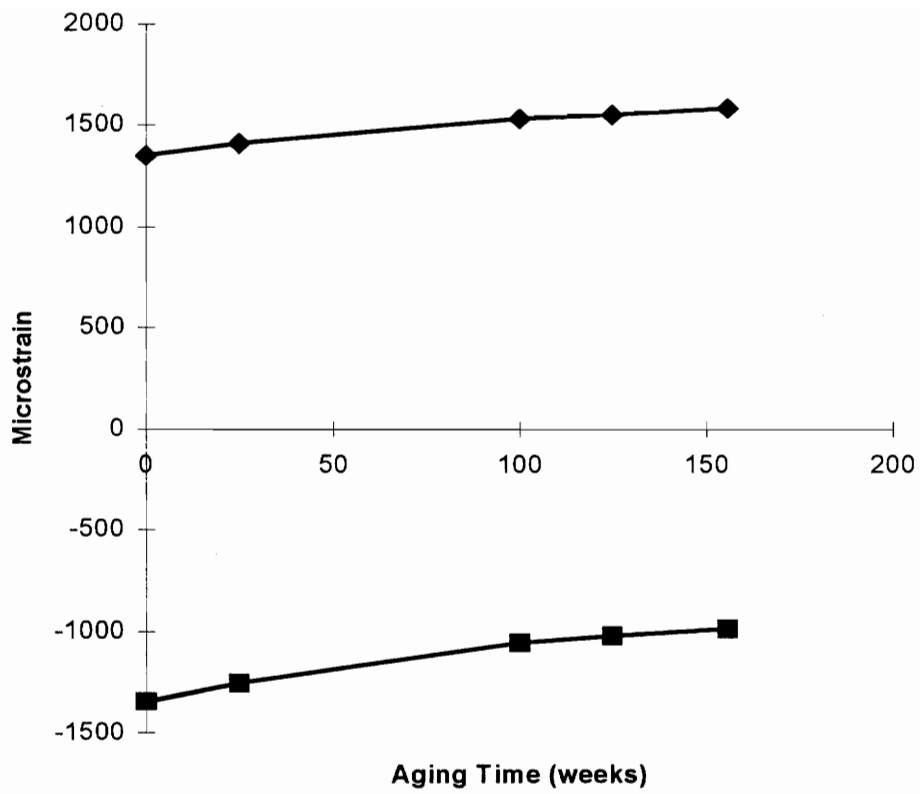


Figure 13 Three year strain history for initially applied strains of $\pm 1350\mu\epsilon$.

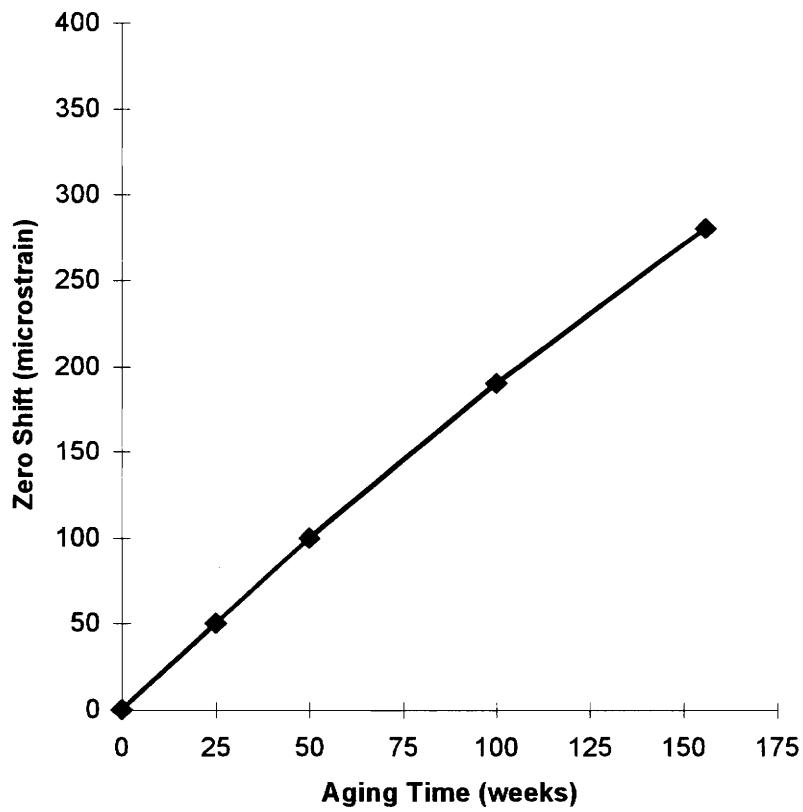


Figure 14 Three year strain history for the unloaded specimens.

creep and gage foil corrosion. Creep decreases the apparent strain magnitude while corrosion adds apparent tensile strain to both tensile and compressively strained beams (Figures 15). Corrosion adds tensile strain by reducing the cross-sectional foil area of the gage which increases the electrical resistance. The magnitude of the strain decline for the 3.170 mm width gage (the same gage width used in this study) adhered to the beam in compression after 3000 hours was less than 100 $\mu\epsilon$. The total strain change, over the three year study period, increased from 280 $\mu\epsilon$ to 370 $\mu\epsilon$ when the initial strain was increased from 780 $\mu\epsilon$ to 1350 $\mu\epsilon$.

Shay's results cannot be directly applied to this study due to the difference in materials examined, aging temperature used, and strain level used. It is however, reasonable to suggest that adhesive creep did contribute to the decline in compressive panel strain observed in this study. The effect of adhesive creep should be greater here than in Shay's study due to the larger applied compressive strain and higher aging temperature. For the reaction rod strain gages, only a small amount of creep, if any, would be expected to occur due to the small amount of strain present in the rods. Gage-foil corrosion should not have affected the measured strain because of the thermal compensation setup which is described in the next section.

Thermal Compensation

As stated earlier, thermal compensation panels were used to subtract out the strains induced by temperature and aging from the panel strain measurements. Differences in the rate of physical aging or chemical aging occurring between the aging panels and the thermal compensation panels could have introduced error into the strain readings. The compressive loading could have affected the rate of physical aging in the stressed panels differently from that of the unstressed thermal compensation panels. Also, the loaded panels were exposed to the oxygen environment (air) on only two edges because they were enclosed in the fixtures. The thermal compensation panels were significantly smaller

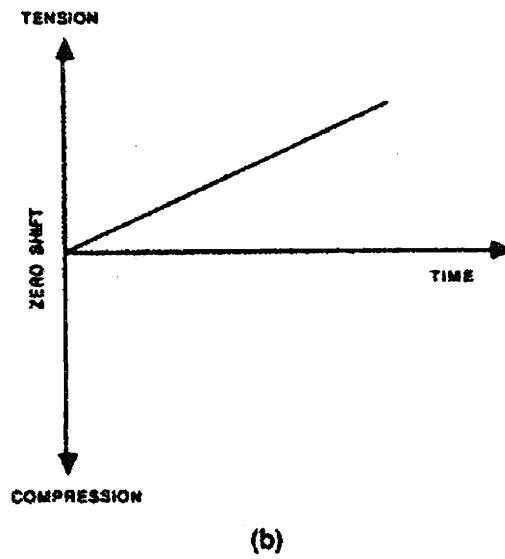
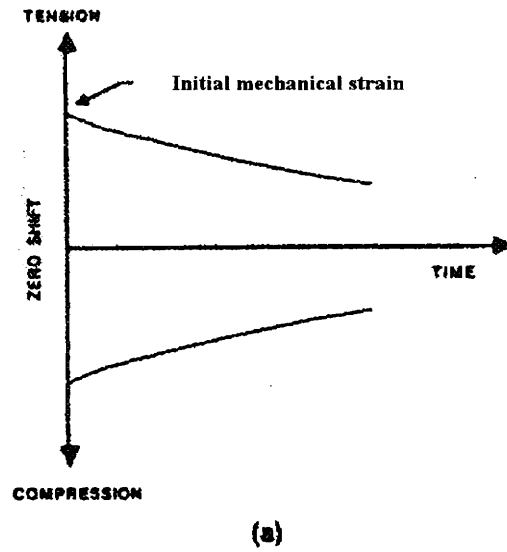


Figure 15 Theorized effects of (a) strain gage adhesive creep and (b) gage foil corrosion on measured electrical strain (Shay).

(about 82% smaller by volume) and exposed to the oxygen environment on all sides. So, oxidation may have occurred faster in the compensation panels than in the loaded panels. Other types of chemical aging may have also been occurring and similarly affecting the stressed panels differently than the unstressed compensation panels.

The expression below describes how the half-bridge strain gage setup is designed to subtract out the thermal strain (ϵ_T) and possible physical (ϵ_{PA}) and chemical (ϵ_{CA}) aging strains measured in the temperature compensation panel (Dummy) from the loaded panel strain (Active):

$$\epsilon_{\text{Panel}} = (- \epsilon_M + \epsilon_T \pm \epsilon_{PA} \pm \epsilon_{CA})_{\text{Active}} - (\epsilon_T - \epsilon_{PA} \pm \epsilon_{CA})_{\text{Dummy}} \quad (1)$$

where ϵ_M is the mechanical strain applied to the composite panel. The (\pm) sign convention was used to distinguish between the potential tensile (+) and compressive (-) strains generated. Considering Shay's results and incorporating adhesive creep and foil corrosion into Expression 1, a new expression for the measured panel strain was created:

$$\epsilon_{\text{Panel}} = (-\epsilon_M + \epsilon_T \pm \epsilon_{PA} \pm \epsilon_{CA} + \epsilon_{\text{Creep}} + \epsilon_{\text{Corrosion}})_{\text{Active}} - (\epsilon_T - \epsilon_{PA} \pm \epsilon_{CA} + \epsilon_{\text{Corrosion}})_{\text{Dummy}}. \quad (2)$$

Creep in the thermal compensation adhesive was neglected since those panels were unloaded and subject only to the small amount of thermally induced strain.

Assuming that the thermal (ϵ_T) and corrosion ($\epsilon_{\text{Corrosion}}$) strains were the same between the active and dummy gages, Expression 2 can be reduced to the following expression:

$$\epsilon_{\text{Panel}} = (- \epsilon_M \pm \epsilon_{PA} \pm \epsilon_{CA} + \epsilon_{\text{Creep}})_{\text{Active}} - (- \epsilon_{PA} \pm \epsilon_{CA})_{\text{Dummy}}. \quad (3)$$

The corrosion strains were canceled since the active and dummy gages were prepared in the same manner and exposed to the same aging environment. Expression 3 suggests that creep of the strain gage adhesive could be the primary cause of the strain decline.

It is difficult to predict what effect physical and chemical aging may have on the strain measurements. If the strains induced by physical and chemical aging are small or the same for both the compressively strained panels and the unstressed thermal compensation panels then their effect would be negligible since the dummy and active strains are subtracted in Expression 3. As mentioned earlier, it is possible that different rates of physical and chemical aging occurred in the compensation panels and the stressed panels. Applied tensile stress is known to increase the free volume present in the polymers. Similarly, chemical degradation creates voids and disorder in the polymer structure which increases free volume. Aging in combination with compressive loading could have different results. For example, chain scission increases voids and free volume while reducing the average molecular weight of the polymer. If compressive loading is added, low molecular weight substances and voids could be forced out of the polymer decreasing the free volume.

For the composite systems studied, it is reasonable to suggest that physical aging may have been slowed by the compressive loading since the setup allowed the following: bending of the composite, Poisson expansion in two directions, potential delamination, and fiber buckling. All the previous could increase the free volume. The potential physical and chemical aging differences between the active and dummy gages mentioned above would create apparent strains that would change the mechanical strain as follows:

$$\epsilon_{\text{Panel}} = -\epsilon_M + \epsilon_{\text{Creep}} \pm \Delta\epsilon_{\text{PA}} \pm \Delta\epsilon_{\text{CA}}. \quad (4)$$

As long as some apparent tensile strain remains between the combined effects of strain gage adhesive creep, physical aging, and chemical aging the panel strain monitored will decrease over time.

The difference in strain decline rate between the IM7/K3B composite and IM7/PETI-5 composite could have been due to the different viscoelastic natures of the two material systems. Creep and stress relaxation of the composite panel would increase the mechanical strain (ϵ_M). After 3000 hours of stressed aging, the creep recovery of both material systems was monitored. IM7/PETI-5 was observed to have a slightly greater amount of creep recovery than IM7/K3B. The magnitudes are not going to be emphasized because temperature effects were not taken into account over the 24-hour recovery period. Also, the creep recovery observed may not have been representative of the creep that occurred during the aging since there could have been some permanent deformation. If IM7/PETI-5 had a faster rate of creep or stress relaxation than IM7/K3B, the panel strain decline rate of IM7/PETI-5 would be less than IM7/K3B since increased compressive mechanical strain ($-\epsilon_M$) reduces the effects of adhesive creep ($+\epsilon_{Creep}$).

Another possibility for the difference in strain decline between the material systems could be that the apparent tensile strain resulting from the combined effects of, strain gage adhesive creep, physical aging, and chemical aging were different for IM7/K3B and IM7/PETI-5. Since K3B is a thermoplastic, physical aging effects would be expected to occur faster in it than in PETI-5 which is a thermoset. The opposite would be true regarding chemical degradation. Faster physical or chemical aging would increase any physical or chemical aging strain difference between the active and dummy gages ($\Delta\epsilon_{PA}$ or $\Delta\epsilon_{CA}$) over the aging period. This could have caused the difference in apparent strain decline rate observed between the IM7/K3B and IM7/PETI-5 material systems aged for 3000 hours.

The rod strains were monitored in a manner similar to the panel strains. A gaged thermal compensation rod subtracted out any thermal or corrosion strains from the rods present in the fixtures. So, the measured rod strain would only change with an actual panel strain change or any strain gage adhesive creep since there was obviously no chemical or physical aging effects present in the steel rods. The magnitude of the resultant rod strain change due to an actual change in panel strain would probably be very small,

due to the high modulus of the steel, and possibly undetectable by the rod strain gages. Also, due to the small magnitude of the rod strains; only small amounts of adhesive creep, if any, would be expected to occur. No observable increase or decrease in the rod strains was seen over the 3000 hours of aging (Figures 10 and 11).

1500-Hour Panels

As mentioned in the experimental section, there were also eight panels aged four at a time for 1500 hours. In the first aging group, four panel-fixture assemblies, two with IM7/K3B panels and two with IM7/PETI-5 panels, and two un-aged temperature compensation panels were conditioned together. In the second group, four panel-fixture assemblies and the same compensation panels previously aged for 1500 hours were conditioned. The individual panel strains and the average change in the rod strain histories for both 1500-hour aging sets are displayed in Figures 16-19.

The IM7/K3B panel strain decline rate for the first 1500-hour aging group was nearly the same as that seen for the IM7/K3B panels aged for 3000 hours (Figures 16-17 and Table 1). The magnitude of the strain decline slope decreased for the second set of IM7/K3B panels. This difference in strain decline rate between the first and second 1500-hour aging group could be the result of physical and chemical aging. Since both types of aging would slow down over time, any strain change due to physical or chemical aging in the aged thermal compensation panel would be less than that of the unaged panels. So, considering physical aging only, if the compensation panel (dummy) shrank over time, the shrinkage would probably be less during the second 1500 hours. Now, if the physical aging strain difference between the active and dummy gage was negligible or zero ($\Delta\epsilon_{PA} = 0$ in Expression (4)) for the first 1500 hours, then for the second 1500 hours $\Delta\epsilon_{PA}$ would

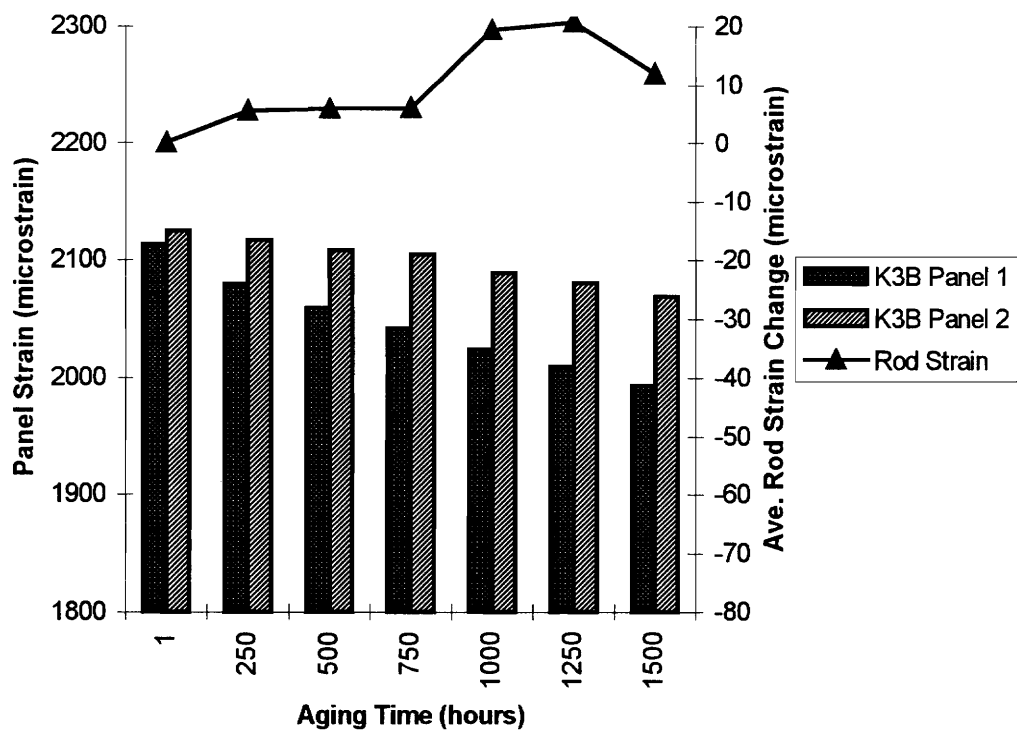


Figure 16 Panel and rod strains for the first IM7/K3B 1500-hour aging.

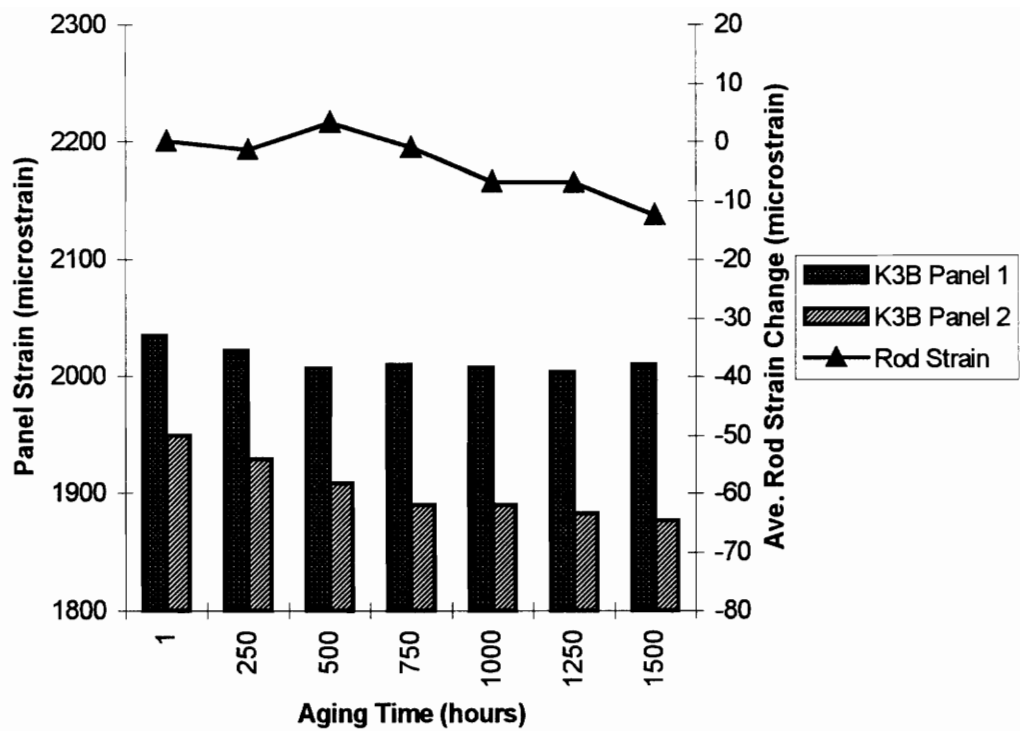


Figure 17 Panel and rod strains for the second IM7/K3B 1500-hour aging.

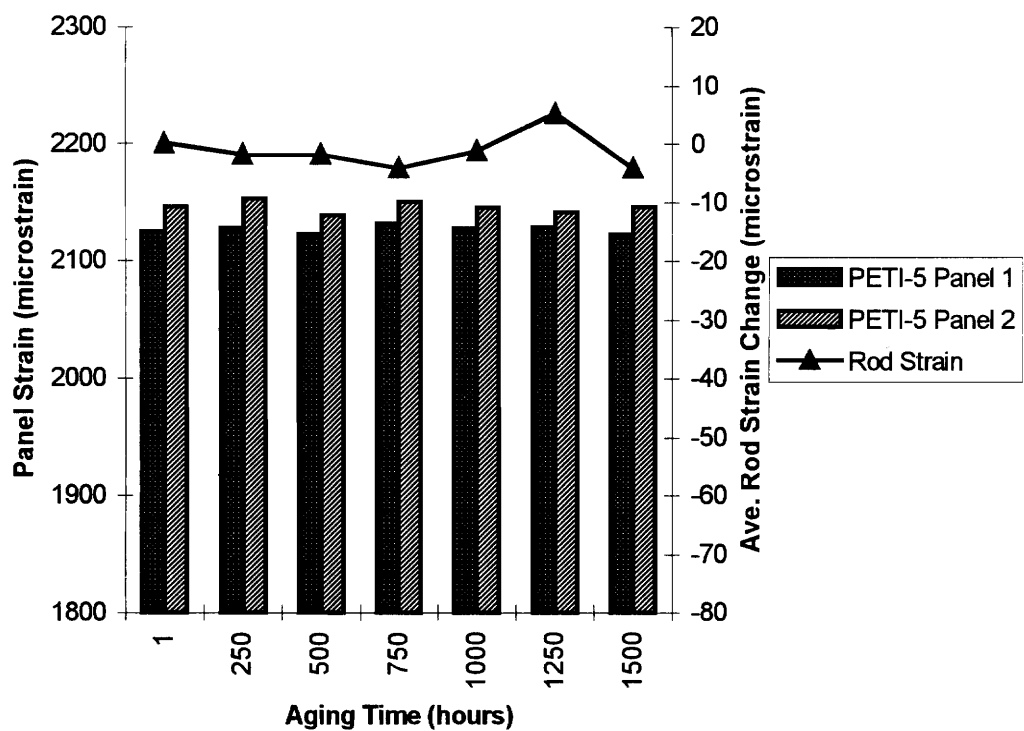


Figure 18 Panel and rod strains for the first IM7/PETI-5 1500-hour aging.

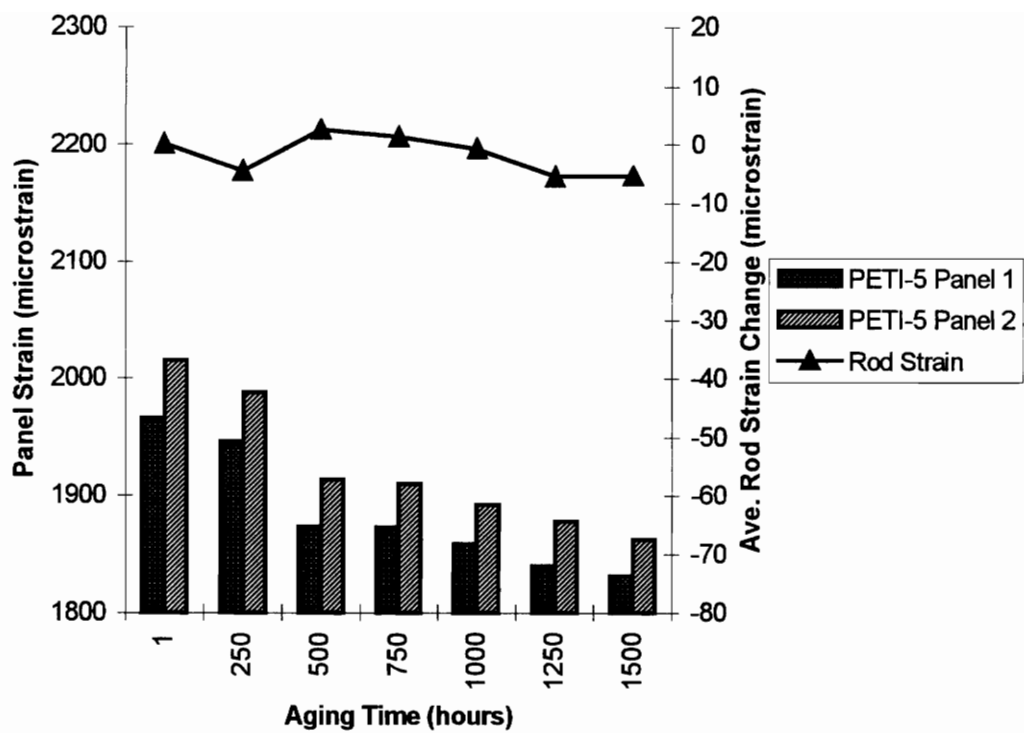


Figure 19 Panel and rod strains for the second IM7/PETI-5 1500-hour aging.

have to be negative. This negative strain difference would reduce the effects of strain gage adhesive creep and decrease the panel strain decline rate as was observed.

The IM7/PETI-5 panel strain (Figures 18-19 and Table 1) for the first 1500-hour aging had almost no slope throughout the aging time. This result is inconsistent with the slope of the 3000-hour IM7/PETI-5 aging. The second 1500-hour IM7/PETI-5 aging had a strain decline that was steeper than both the first 1500-hour and 3000-hour IM7/PETI-5 aging. It is suspected that the strain measurements of the IM7/PETI-5 composites were inaccurate, possibly due to poor strain gage application or bad wiring of the temperature compensation panel. This was concluded because these results are so different from the larger IM7/PETI-5 test group aged for 3000 hours and the slope change from the first 1500-hour aging to the second was so extreme.

Compression Tests

A typical stress versus strain curve for an IM7/K3B and an IM7/PETI-5 specimen is displayed in Figures 20-21. Radiograph images of compressed specimens showed no damage at stress levels around 95% of the ultimate compressive stress. The radiographs confirmed classical lamination theory estimates that predicted failure of the 0°-plys first just prior to laminate failure. The gage section of the stressed specimens were also polished and viewed under a microscope. This analysis also showed no evidence of damage. A stress versus strain curve for one of the IM7/PETI-5 specimens stressed to 85% of the panels ultimate compressive stress is displayed in Figure 22. It can be seen in Figure 22 that the curves approach zero strain, during unloading, with no apparent change in modulus. This suggests that no significant laminate damage occurred as a result of the prior loading.

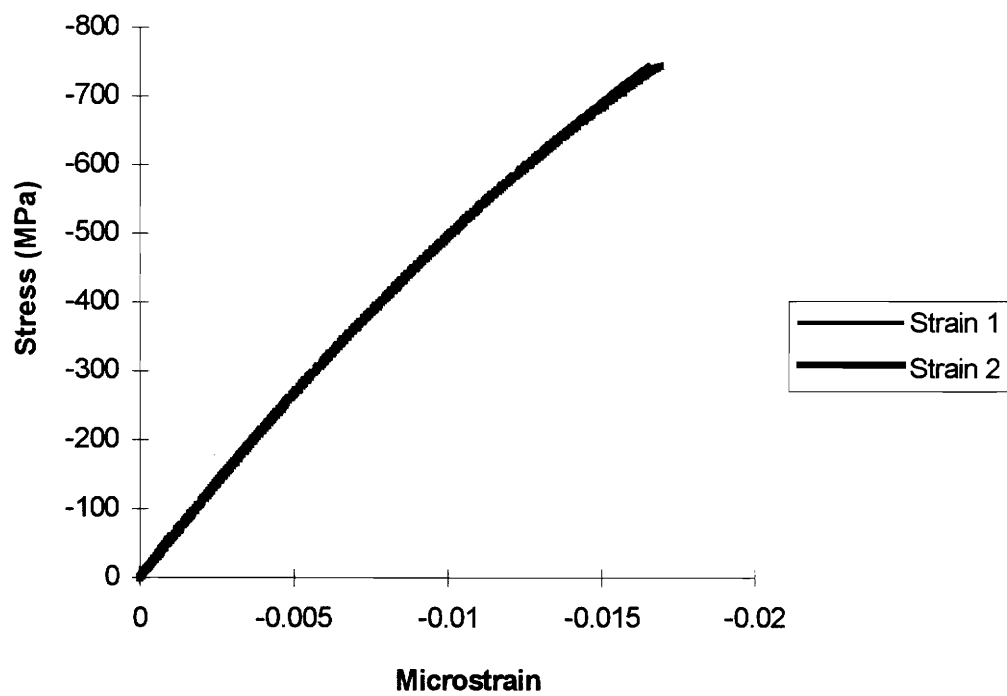


Figure 20 Stress versus strain for an IM7/K3B specimen.

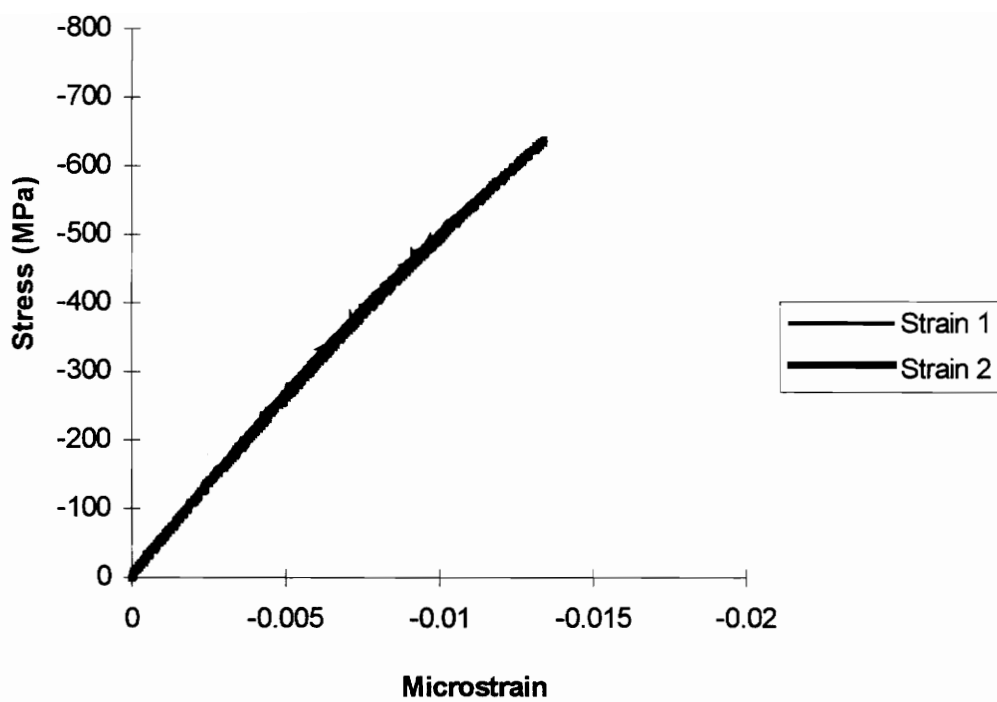


Figure 21 Stress versus strain for an IM7/PETI-5 specimen.

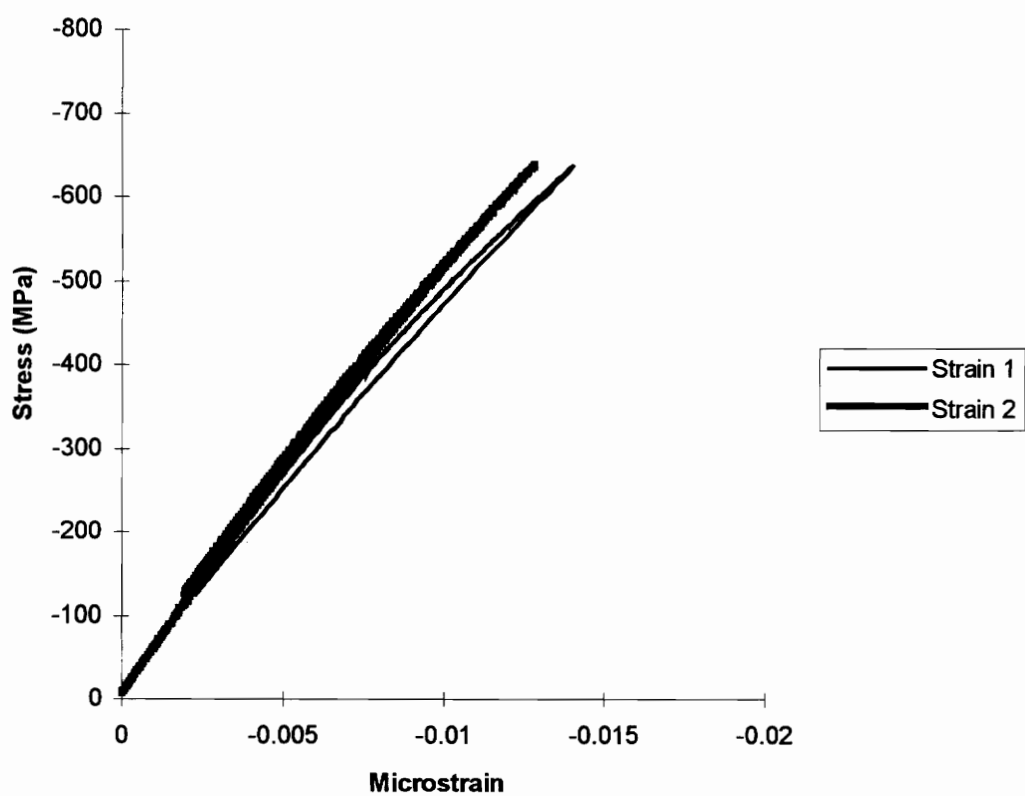


Figure 22 Stress versus strain for an IM7/PETI-5 specimen stressed to 85% of it's ultimate compressive stress.

Only small changes in the average Weibull residual elastic modulus and strength over the 3000-hour aging period was seen in either material system (Figures 23-24). The modulus of both materials was about 52 GPa and remained essentially constant with aging time (Tables 2-3). Initially, the IM7/K3B composite possessed about a 15% higher residual strength than the IM7/PETI-5. With aging, the IM7/K3B mean strength was almost unchanged except for a small increase between the first and second aging time. The IM7/PETI-5 composite showed a progressive decrease in strength, 633 MPa to 610 MPa, over the 3000-hour aging. No significant trend was seen for the strain at failure values. The modulus and strength values will be examined more closely in the statistical analysis section.

Statistical Analysis

The significance between data of various aging conditions and material systems was assessed using Dunn's procedure [41]. This tool provides a method to compare medians at a given level of confidence. First, the Kruskal-Wallis one-way analysis of variance by ranks [41] was used to test the null hypothesis that the population distribution functions were identical. If the hypothesis was accepted, then the distributions (and likewise the means or medians) of the populations were the same. If the hypothesis was rejected, then Dunn's multiple-comparison procedure was applied to determine which medians were the same. The Kruskal-Wallis test was used with a significance level of 0.05 ($\alpha = 0.05$). For Dunn's test, an error rate (similar to level of confidence) of 0.15 was chosen to be three times the alpha value used for the dual comparison test.

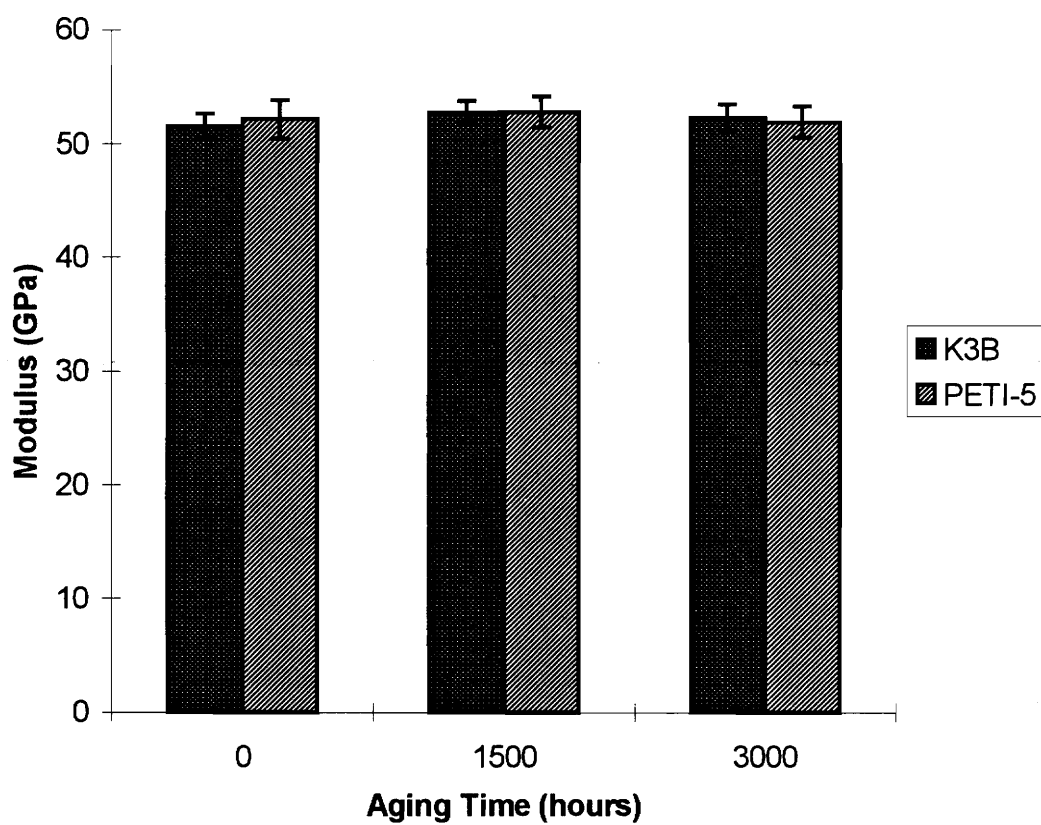


Figure 23 Quasi-static modulus versus aging time.

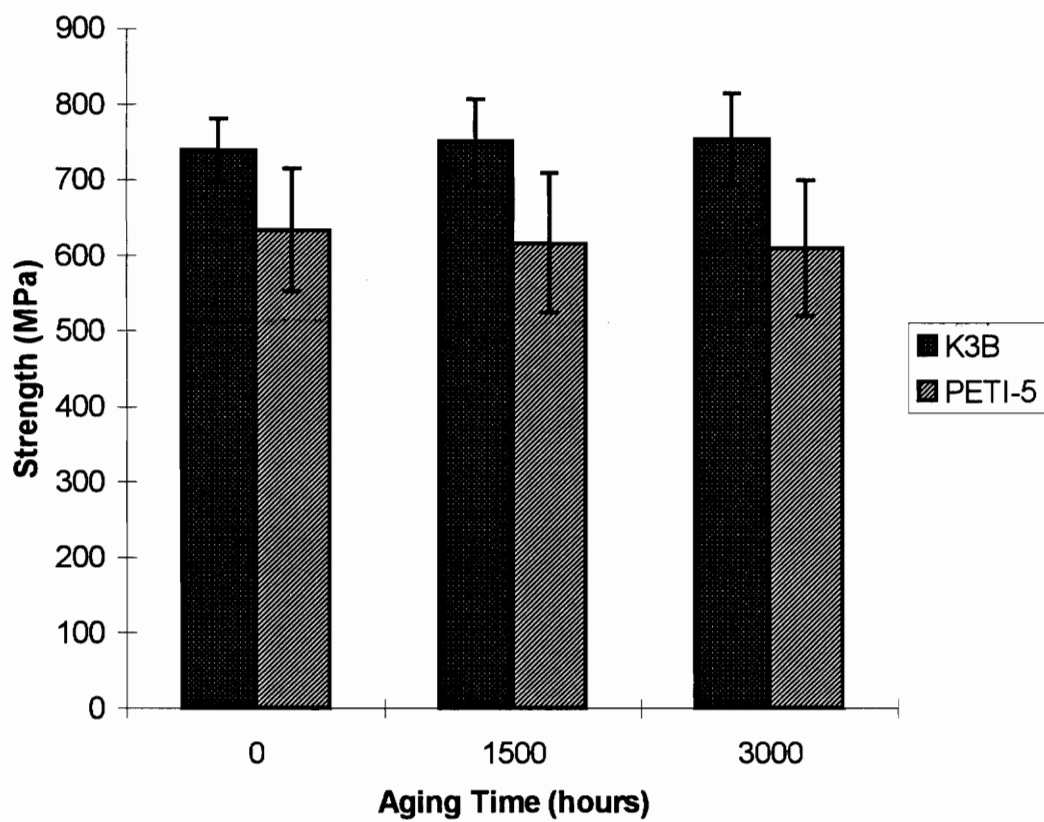


Figure 24 Quasi-static strength versus aging time.

Table 2 IITRI compression results for the IM7/K3B composite.

Age	Modulus (GPa)	Strength (MPa)	Strain at Failure	Number of Specimens
Baseline	51.55 ± 1.11	738.5 ± 42.2	0.0172 ± 0.0015	17
1500	52.75 ± 1.05	750.0 ± 56.7	0.0168 ± 0.0018	18
3000	52.28 ± 1.20	753.3 ± 60.5	0.0171 ± 0.0018	18

Table 3 IITRI compression results for the IM7/PETI-5 composite.

Age	Modulus (GPa)	Strength (MPa)	Strain at Failure	Number of Specimens
Baseline	52.16 ± 1.73	633.4 ± 81.0	0.0135 ± 0.0022	19
1500	52.83 ± 1.37	616.4 ± 92.3	0.0129 ± 0.0025	18
3000	51.96 ± 1.36	609.5 ± 89.5	0.0132 ± 0.0022	17

Results of the statistical analysis comparison determined that the moduli values did not differ between the different aging times for the individual material systems or between the two material systems at a particular aging time. The one exception was that the median modulus value of the IM7/K3B baseline material was determined to be statistically lower than that of the IM7/K3B 1500-hour material. However, it was statistically identical to the IM7/K3B 3000-hour median. This is a result of the stringent confidence level chosen. The IM7/K3B strength was determined to be greater than the IM7/PETI-5 strength at every aging time. When the three aging times were compared for both material systems separately, the results showed that the different age strength populations were the same.

A Weibull analysis was used to calculate mean, standard deviation, shape parameter (α), characteristic value (β), observed significance level, A-basis and B-basis allowables. These numbers have been tabulated in Tables 2-5. The Weibull equations used are listed in Appendix A. The observed significance level (OSL) is based on the Anderson-Darling goodness-of-fit statistics [42]. For Anderson-Darling the hypothesis is that the samples tested are taken from Weibull distributions with the listed value of the parameters. Since all of the OSL values are greater than 0.05, the hypothesis is not rejected. The A-basis allowable number is the value above which at least 99% of the population of values is expected to fall, with a confidence level of 95%. Similarly, the B-basis allowable represents a reliability of 90% with a confidence level of 95%. The low allowable for the IM7/PETI-5 strength, resulting from the low alpha value, is directly related to the low average strength seen in several blanks.

It is apparent from Tables 4 and 5 that the A and B-basis allowables for strength are decreasing with conditioning time. The decrease is the result of increased scatter in the data which lowers the alpha value used in calculating the allowables. This trend is most apparent between the baseline and aged 1500 hour material. There is almost no difference between the 1500-hour and 3000-hour IM7/PETI-5 aging times. The cumulative probability of failure versus applied stress plots for the two composite systems

Table 4 Weibull statistics for the IM7/PETI-5 composite.

Weibull Statistic	Modulus (GPa)			Strength (MPa)		
	Baseline	1500 Hours	3000 Hours	Baseline	1500 Hours	3000 Hours
Alpha	37.96	48.60	48.30	9.37	7.92	8.09
Beta	52.93	53.45	52.56	667.7	654.8	646.9
OSL	0.285	0.146	0.343	0.731	0.090	0.133
Mean	52.16	52.83	51.96	633.4	616.4	609.5
A-Allowable	46.47	48.27	47.44	394.1	350.6	350.4
B-Allowable	49.44	50.66	49.80	506.4	471.7	468.5

Table 5 Weibull statistics for the IM7/K3B composite.

Weibull Statistic	Modulus (GPa)			Strength (MPa)		
	Baseline	1500 Hours	3000 Hours	Baseline	1500 Hours	3000 Hours
Alpha	58.83	63.64	55.14	21.77	16.29	15.27
Beta	52.04	53.22	52.81	757.0	774.7	779.6
OSL	0.238	0.3859	0.138	0.721	0.591	0.459
Mean	51.55	52.75	52.28	738.5	750.0	753.3
A-Allowable	47.84	49.24	48.28	602.9	571.8	563.9
B-Allowable	49.79	51.09	50.38	671.6	660.5	657.6

(Figures 25-26) show graphically how the strength distributions change over time. For the IM7/K3B composite, the strength distribution (Figure 25) broadens such that for a given strength the probability of attaining that strength decreases. The trend over time of the IM7/PETI-5 composite (Figure 26), although small, appears to shift to lower strengths. Comparing the two figures, IM7/PETI-5 possesses a broader distribution in scatter than IM7/K3B.

Differential Scanning Calorimetry

The results from the DSC analysis are displayed in Table 6. Scan 2 was completed immediately following a quench of the first scan. A third scan was also performed in order to verify that the sample had been rejuvenated as much as possible by the first scan. As expected, the results of the third scans were nearly identical to the second for every sample tested. The glass transition value reported was the inflection point of the heat flow versus temperature curve as calculated by the DuPont software. From Table 6, it appears that there was no significant change in the glass transition temperature as a result of the aging for IM7/K3B. For IM7/PETI-5, it is difficult to deduce the effects aging since the glass transition temperature in the first scan was hard to detect. There doesn't appear to be any irreversible change in the glass transition temperature, due to aging, for either material system since the second scan was nearly the same at every aging time including the baseline. Many of the first scans on the IM7/PETI-5 composite do not have a T_g value reported because their transition region was very broad and did not possess a significant inflection.

In Figures 27-28, the four DSC curves displayed are first scans of the unaged, aged 1500 hour, aged 3000 hour, and aged 3000 hour without stress materials. It appears that for the IM7/PETI-5 material (Figure 27) the endothermic drop in heat flow becomes

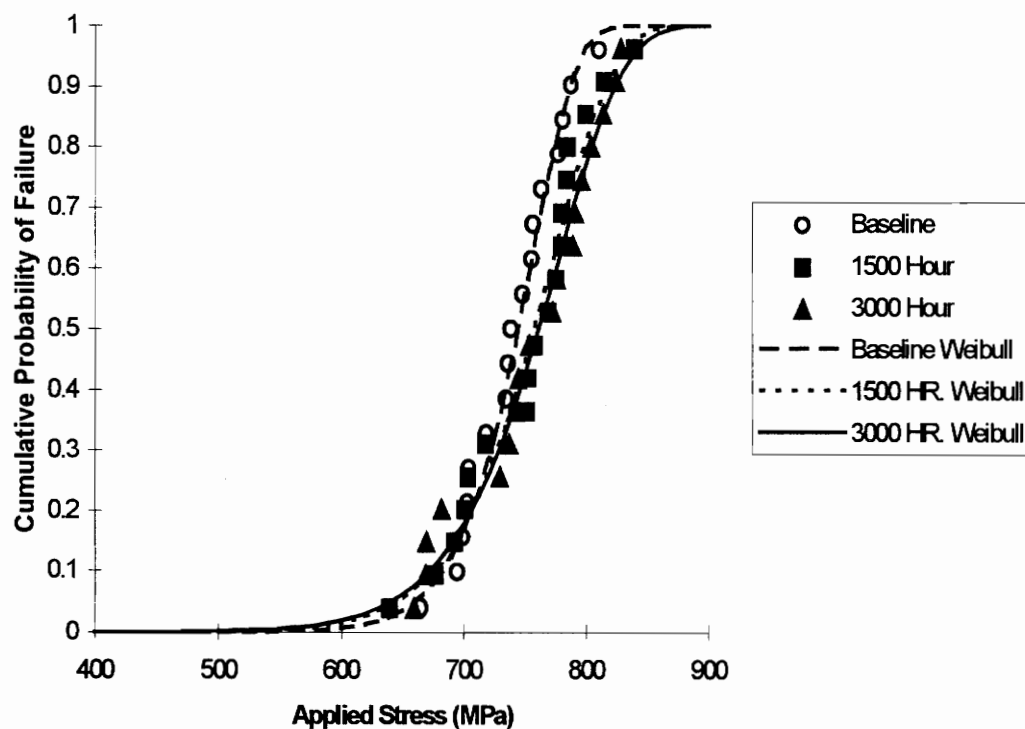


Figure 25 Weibull strength distribution for the IM7/K3B composite.

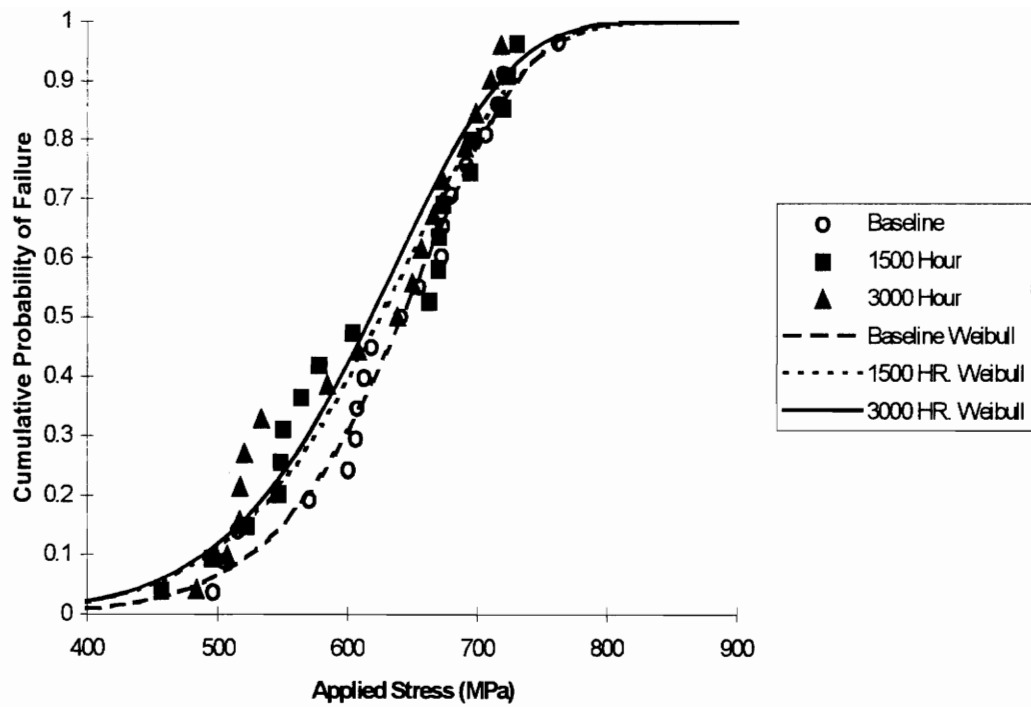


Figure 26 Weibull strength distribution for the IM7/PETI-5 composite.

Table 6 Glass transition temperature as determined by DSC.

Age	Sample	IM7/K3B		IM7/PETI-5	
		Glass Transition Temp. (°C)		Glass Transition Temp. (°C)	
		Scan 1	Scan 2	Scan 1	Scan 2
0	A	227	239	244	255
	B	231	234	244	259
1500	A	224	236	243	258
	B	226	238	253	263
3000 Stress	A	225	233	--	259
	B	223	236	--	261
3000 No Stress	A	224	236	--	256
	B	225	236	--	259

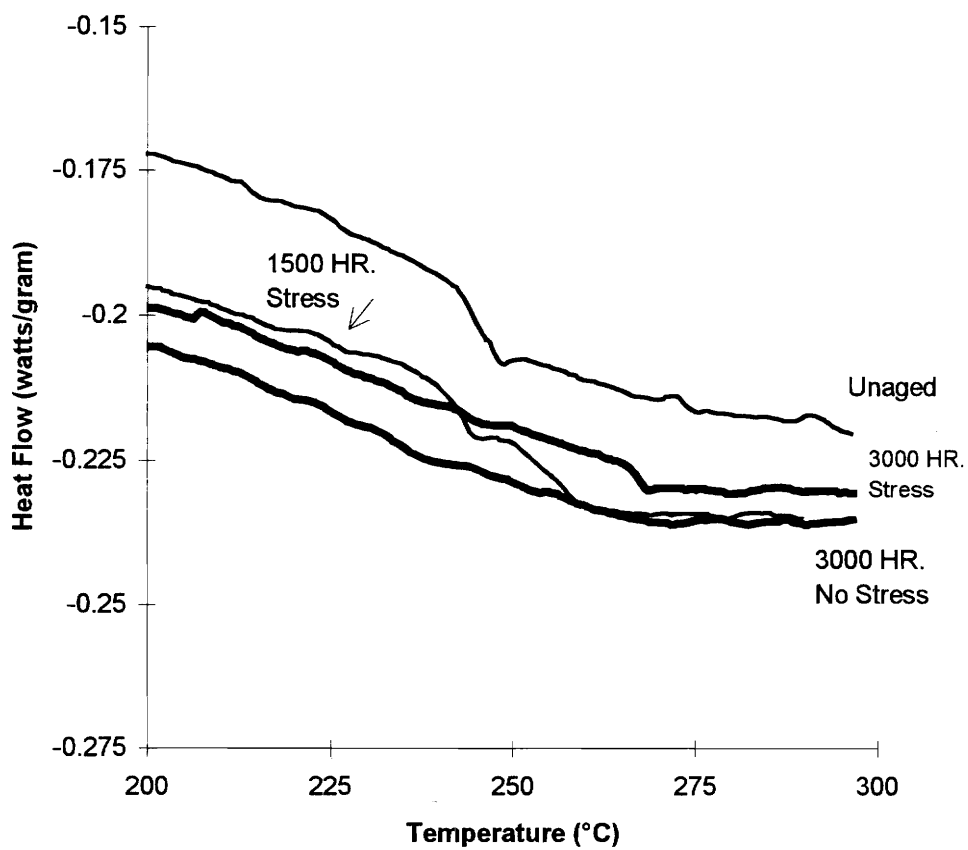


Figure 27 DSC scans on IM7/PETI-5 for four aging conditions.

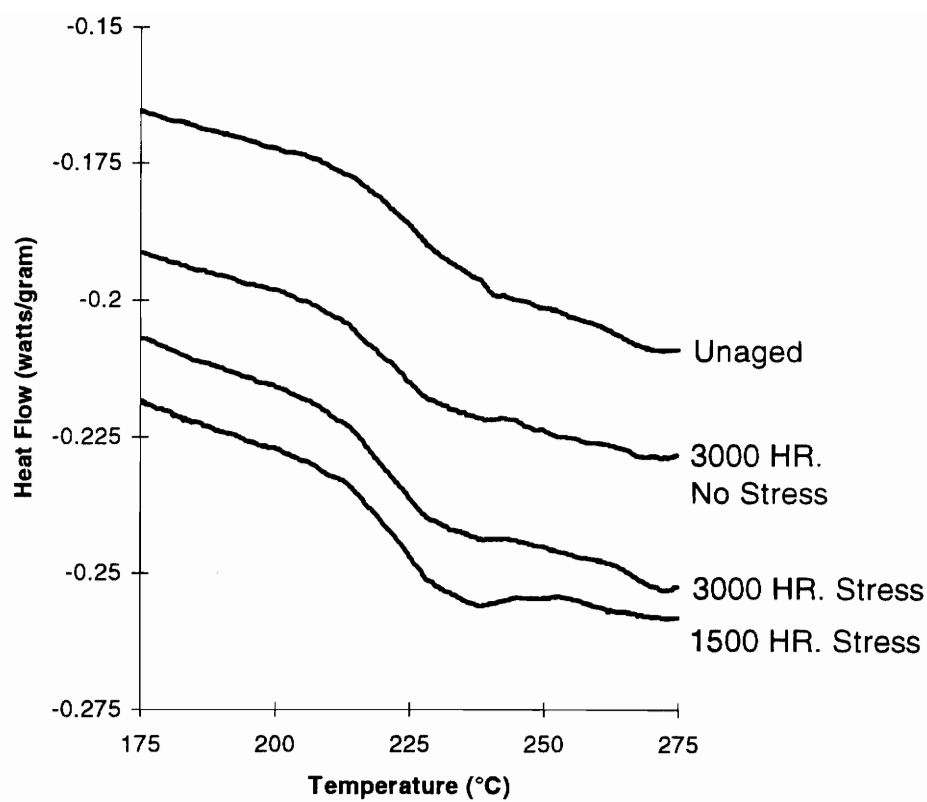


Figure 28 DSC scans on IM7/K3B for four aging conditions.

broadened with aging. For both the stressed and unstressed IM7/PETI-5 samples aged for 3000 hours, the glass transition inflection point in the first scan was undetectable due to the increased broadness of the endothermic drop. A similar trend is not apparent for the IM7/K3B curves (Figure 28).

Looking at the different DSC scans for the IM7/PETI-5 thermal dummy aged for 3000 hours (Figure 29), it appears that the broad (almost linear) transition is only present in the first scan. A similar trend was seen in the 3000-hour stressed specimen (Figure 30). Again, this was not seen for the IM7/K3B material (Figure 31). The broad IM7/PETI-5 glass transition region could be a result of the processing of the composite which restricts polymer chain movement since all of the first scans were broad. The slight increase in broadness with aging may be the result of physical aging which would reduce free volume and further restrict chain movement within the polymer, potentially broadening the glass transition region. This physical aging effect would be reversible and may also affect the crosslinked PETI-5 polymer before the linear K3B polymer.

In all of the DSC tests performed, the first scan consistently produced a lower glass transition temperature than the second and third scans (Table 6). This is the opposite of what normally occurs as a result of physical aging. Crystallization occurring during the first quench could raise the T_g observed in the second and third scan, but this is unlikely to occur in these particular polymers. Chemical degradation during the aging could possibly lower the T_g , but the effect would not be reversible and would not explain the difference between the first and second scan of the unaged material.

One possible explanation for the increase in T_g is if additional curing occurred during the first scan. Additional curing would increase the polymers molecular weight which would then increase the glass transition temperature for the second scan. A 20°C increase in T_g was observed by Hergenrother [38] after an isothermal hold at 400°C on the unaged bulk PETI-5 polymer. The additional curing would also produce an exothermic peak after the glass transition in the first scan. However, no significant increase in heat flow was observed for samples tested. Another possible cause for the increase in T_g is if

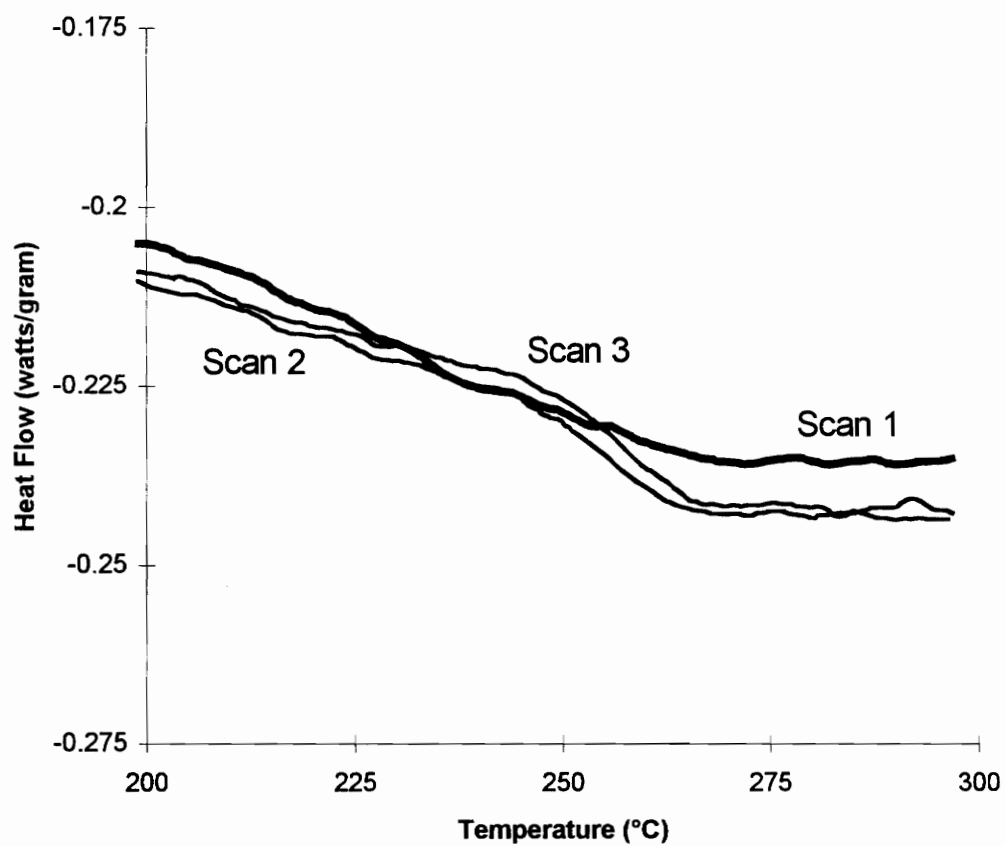


Figure 29 DSC scans on one IM7/PETI-5 sample aged for 3000 hours without compressive loading.

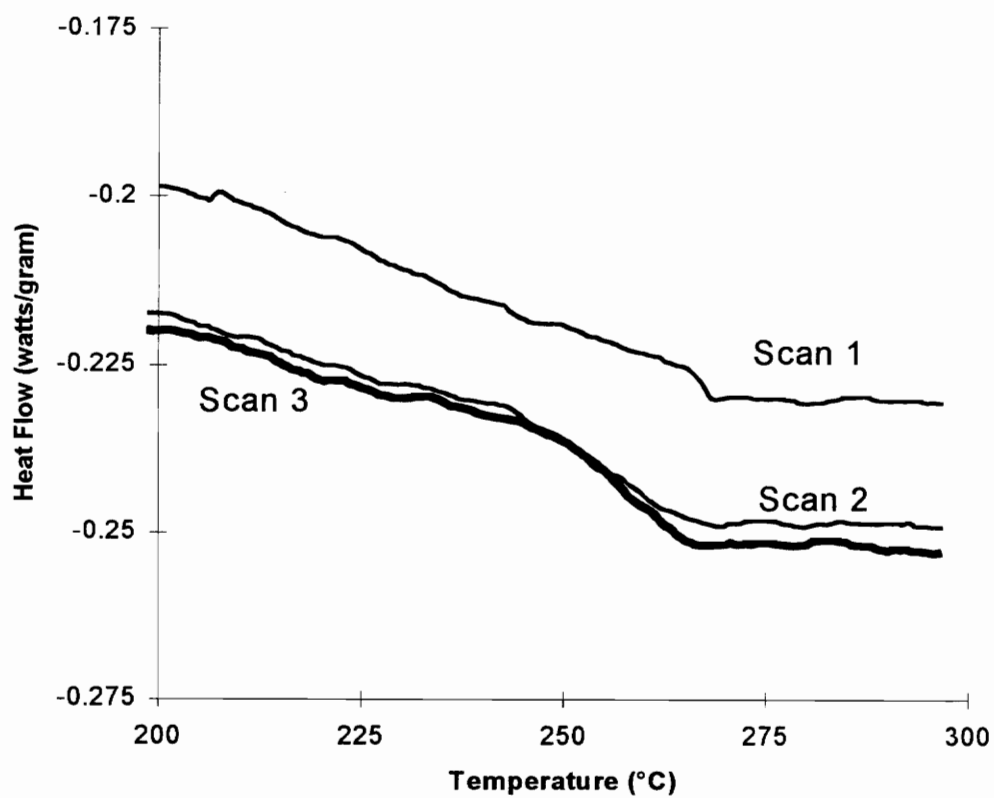


Figure 30 DSC scans on one IM7/PETI-5 sample aged for 3000 hours with compressive loading.

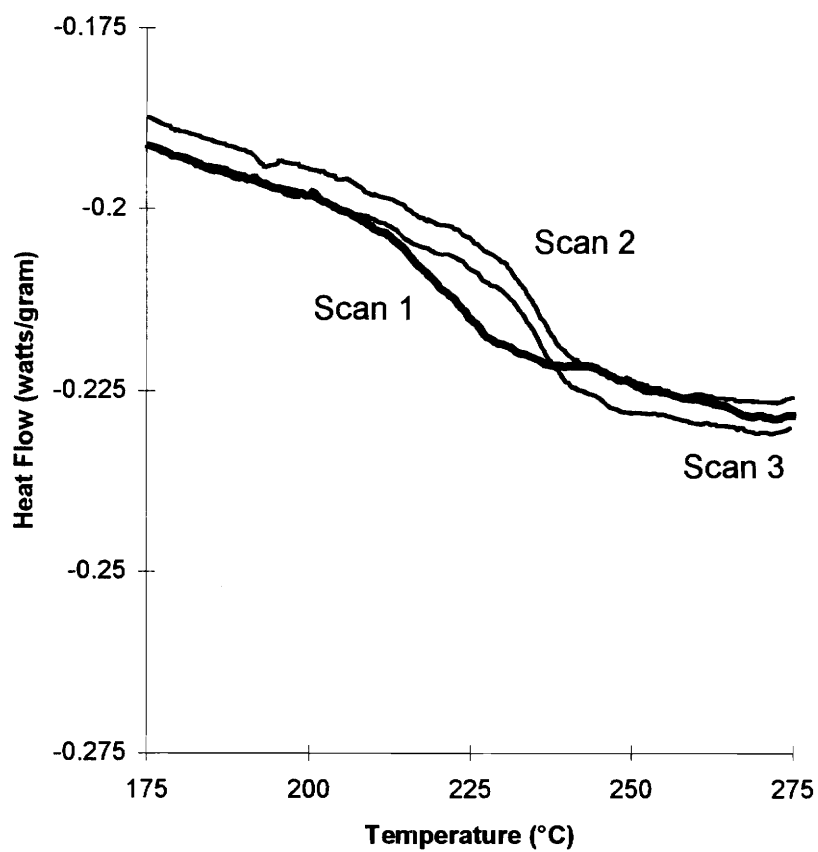


Figure 31 DSC scans on one IM7/K3B sample aged for 3000 hours without compressive loading.

the laminate processing procedure created free volume in the polymer. The additional free volume would then lower the T_g in first scan as observed.

Thermogravimetric Analysis

Because of the sensitivity of thermogravimetric measurements to various experimental factors such as, humidity and airflow rate, the result from one test was only compared to results of tests performed on that same day. The first set of thermogravimetric analysis was performed on two samples from each material system for three different conditions: unaged, aged 3000 hours under stress, and aged 3000 hours without stress. A typical percent weight loss versus temperature curve and its derivative for IM7/K3B and IM7/PETI-5 are displayed in Figures 32-33. The first peak observed in the derivative is believed to be a particular degradation event. For example, the first peak in the IM7/PETI-5 derivative is suspected to be caused by benzene end groups breaking off in combination with other chemical reactions. The peak values and their corresponding temperatures as well as the degradation onset temperatures have been tabulated (Tables 7-8). The degradation onset temperature is the temperature corresponding to a weight loss rate of 0.025%/min.

It appears that the first peak of the weight loss rate curve for IM7/K3B becomes smaller and shifts slightly to lower temperatures with aging time (Figure 34). The thermal compensation peak is the lowest of all three. The smaller peak could be the result of oxidation that occurred. Oxidation, during aging, might degrade some of the polymer decreasing the degradation rate in first TGA derivative peak. If this is true, then it confirms that the temperature compensation pieces experienced more oxidation than the compressed panels. The IM7/PETI-5 TGA curves did not have a significant difference in

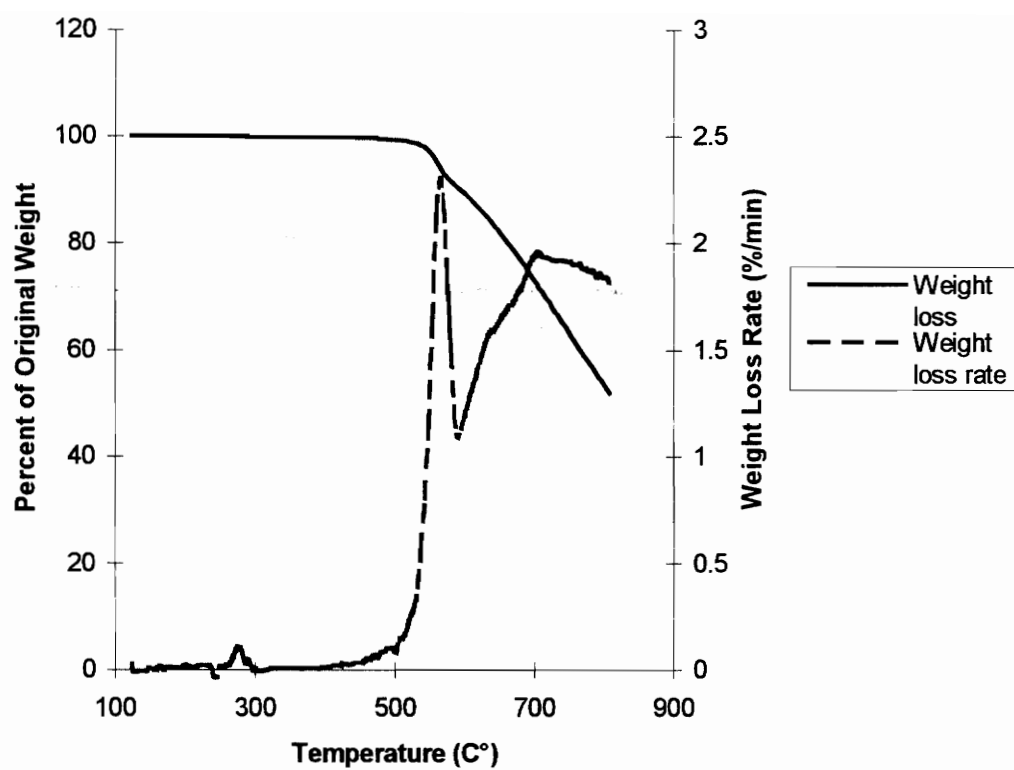


Figure 32 TGA for unaged IM7/K3B.

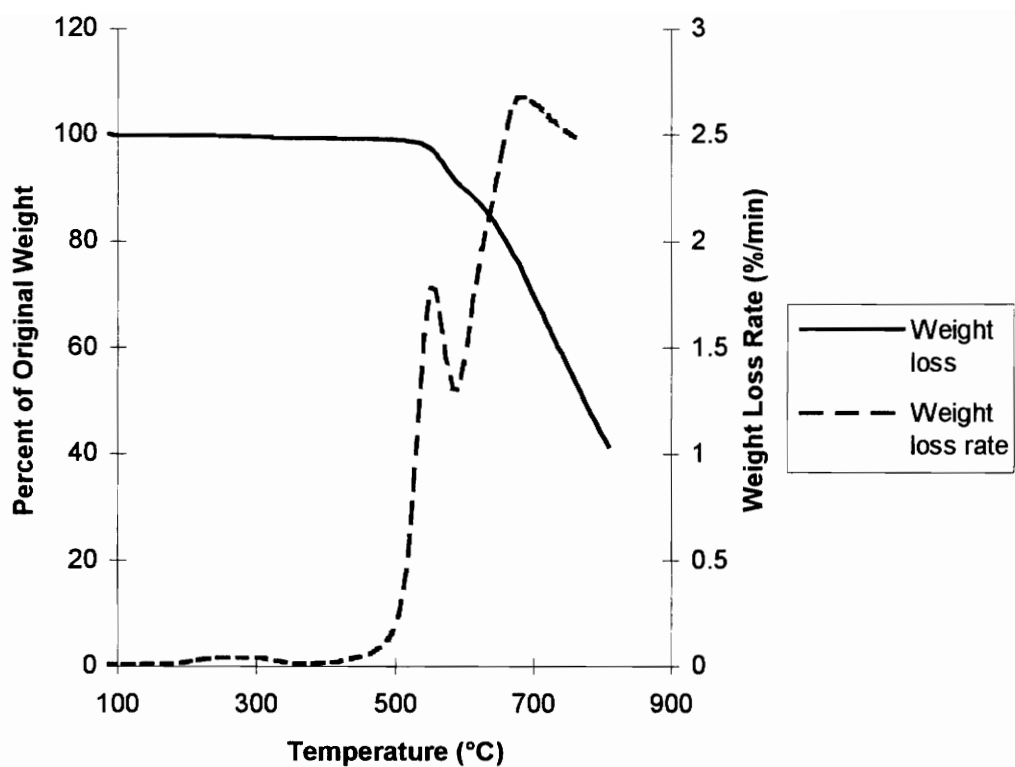


Figure 33 TGA for unaged IM7/PETI-5.

Table 7 TGA results for the IM7/K3B composite.

Age	Degradation Onset	1st Peak	
	Temp. (°C)	Temp. (°C)	Wt. Loss Rate (%/min)
0	522.0	563.3	2.26
3000 Stress	519.8	562.0	2.04
3000 No Stress	520.5	561.0	1.99

Table 8 TGA results for the IM7/PETI-5 composite.

	Degradation Onset	1 st Peak	
Age	Temp. (°C)	Temp. (°C)	Wt. Loss Rate (%/min)
0	529.5	575.0	2.01
3000 Stress	532.8	577.5	2.08
3000 No Stress	534.0	578.6	1.97

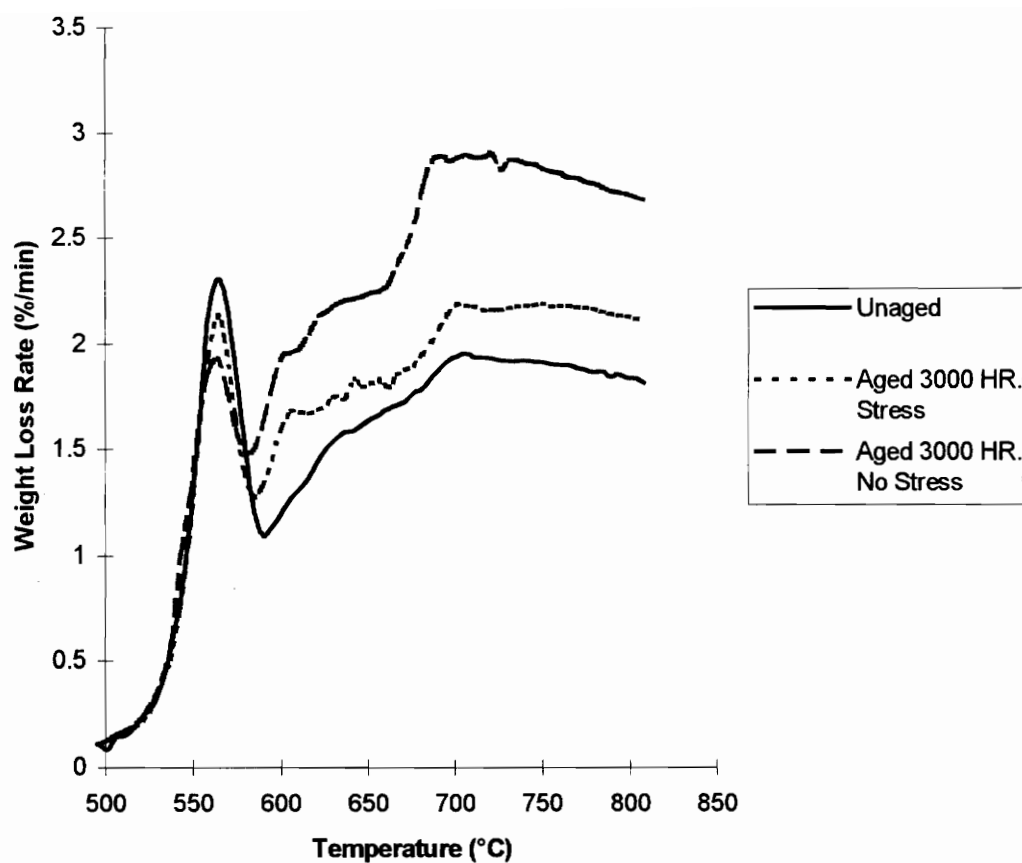


Figure 34 TGA weight loss rate versus temperature for unaged, aged 3000 hours with stress, and aged 3000 hours without stress IM7/K3B samples.

first peak value as a result of the aging (Figure 35). This could signify better thermal stability of the PETI-5 polymer over K3B.

A second set of thermogravimetric analysis was performed to try and confirm that the changing K3B degradation behavior was a result of the thermal mechanical aging. Again, TGA was performed on three samples for each condition: unaged, aged 3000 hours under stress, and aged 3000 hours without stress. Two K3B samples aged for 1500 hours under stress were also examined. The peak value of the derivative of weight loss for each sample was then tabulated and averaged according to its aging condition. These results, including the standard deviation, are displayed in Figure 36 (Note: 3000D represents the thermal dummy aged for 3000 hours). From the figure, it does appear that the unaged sample typically possesses the largest weight loss rate peak. Due to the large standard deviation for the 1500-hour samples, it is difficult to determine if the peak value progressively decreases with thermal mechanical aging. More tests need to be run in order to determine the actual trend with aging.

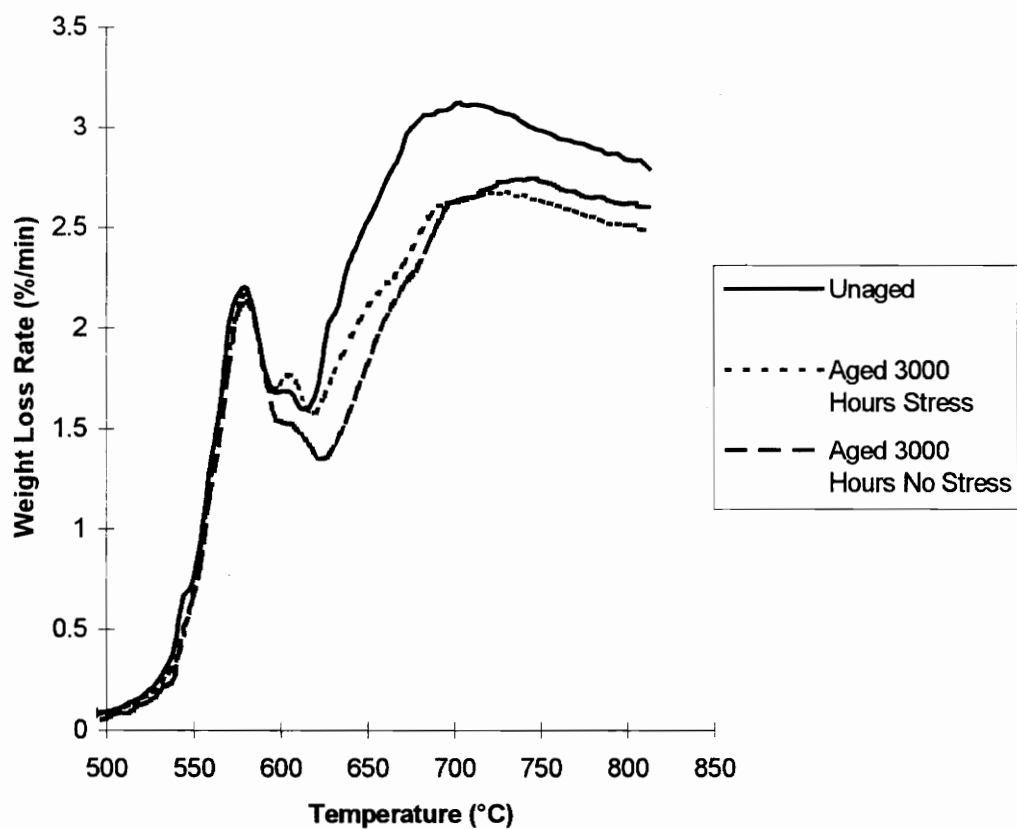


Figure 35 TGA weight loss rate versus temperature for unaged, aged 3000 hours with stress, and aged 3000 hours without stress IM7/PETI-5 samples.

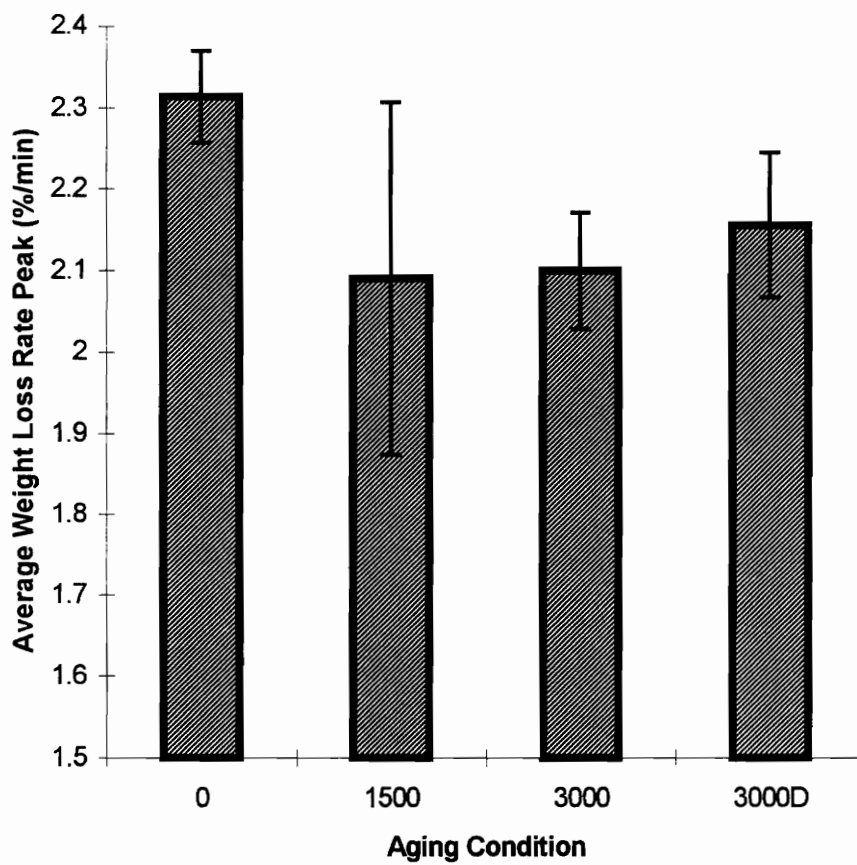


Figure 36 Average derivative of weight loss rate and standard deviation for the four different aging conditions.

IV. SUMMARY AND CONCLUSIONS

Summary of Experimental Procedures

The purpose of this section is to present a concise summary of the materials examined and experimental techniques used in this investigation. This outline will follow the order in which the material was discussed in the report.

Material

- Two carbon fiber-reinforced polyimide material systems were examined in this study, IM7/K3B and IM7/PETI-5. The IM7/K3B composite was processed at The Boeing Company. The IM7/PETI-5 composites were cured by Northrop-Grumman Corporation from prepreg furnished by NASA-Langley. The 16-ply composites had quasi-isotropic laminate configurations, $[+45/-45/0/90]_{2S}$ for IM7/K3B and $[+45/0/-45/90]_{2S}$ for IM7/PETI-5.

Environmental Conditioning

- The Boeing Company provided stainless steel fixtures used to compressively strain the composite panels which were aged at 163°C for up to 3000 hours. The future goal is to continue the aging out to 10,000 hours.
- Strain in the aging composites, as well as the steel reaction rods, was monitored using high temperature strain gages (WK-125-AD-350). The gages were protected from the thermal aging environment by applying an extra coat of high temperature adhesive over the strain gage and solder joint.
- Changes in stiffness or strain in the thermal aging test fixture, panel and reaction rods were monitored by recording the strain every 250 hours. To prevent drift in the system, the strain gage circuit was balanced and calibrated between the weekly readings.

Specimen Preparation

- For the IITRI compression tests, untapered glass/epoxy tabs were adhered to the composite panels to reduce stress concentrations induced from gripping the specimen. The tabs were ground to make them flat and parallel to the plane of the panel. This ensured that the out of plane alignment of the panel was true to the loading axis.

Mechanical Tests

- IITRI quasi-static compression tests were performed under the guidance of ASTM D3410M-94 procedure B. Room temperature displacement controlled tests were performed using a displacement rate of 1 mm/min on a 150 kN screw driven Instron machine. Load and strain signals were recorded using a LabView data acquisition system.

- DSC was performed on a DuPont 910 differential scanning calorimeter. ITCA standard method was used with a heating rate of 10°C/min to heat the sample from 150° to 300°C. The glass transition temperature recorded was the inflection point of the heat flow versus temperature curve.
- TGA used a DuPont 951 thermogravimetric analyzer with a heating rate of 10°C/min and an air flow rate of 40 cc/min. Weight loss rate versus temperature data was acquired and compared between the different age materials.

Summary of Experimental Results and Discussion

In this section, the findings of the experimental work performed in this investigation are summarized and conclusions are made.

Applied Aging Strain

3000-Hour Panels

- This study successfully applied a static compressive load to aging composite panels with less than a 10% variation in strain over 3000 hours.
- The panel strain observed over the 3000 hour aging period decreased 100µε for the IM7/PETI-5 material and 200µε for the IM7/K3B material. The drop in strain was attributed mainly to creep of the strain gage and strain gage adhesive. The difference in strain decline rate between the two material systems was believed to be the result of the different viscoelastic properties of the two material systems.

1500-Hour Panels

- The composite panels aged for 1500 hours also showed a decline in panel strain over the aging period. The first two IM7/K3B panels aged had a strain decline trend similar to the IM7/K3B 3000 hour panels. The second two had a significant decrease in the strain decline rate. The decrease was attributed to reusing the thermal compensation panels previously aged for 1500 hours. The aged thermal compensation panels would have slower rates of physical and chemical aging than the panels just beginning their aging. This difference in strain between the thermal compensation and active strains would affect the strain decline rate, possibly decreasing it as explained in Chapter 3. For the PETI-5 panels, the strain behavior was unexpected. A large increase in panel strain decline rate was observed between the first and second pair of aging panels. The reason for this behavior is unknown.

Compression Tests

- Results of the IITRI compression tests showed that no significant change in stiffness occurred as a result of the 3000 hours of aging at 163°C under compressive loading. Only small decreases in strength were observed.
- The IM7/K3B and IM7/PETI-5 laminates possessed similar moduli values. The mean strength of IM7/K3B was significantly higher than that of IM7/PETI-5, approximately 15% higher.

Statistical Analysis

- Statistical analysis, specifically Kruskal-Wallis one-way analysis of variance and Dunn's multiple comparison procedure, was performed on the modulus and strength results. It was determined that the moduli values did not differ between the two

material systems at any aging time. The moduli values were also found not different between aging times of a particular material system. There was one exception; the IM7/K3B baseline median modulus was determined to be lower than the IM7/K3B 1500-hour median modulus. The strength comparison found IM7/K3B to be stronger than IM7/PETI-5 at every aging time. The comparison between aging times determined that the median strength values for the two material systems did not differ with aging time.

- Weibull statistical analysis was used to calculate means, standard deviations, and allowables. There was a slight decline in the strength allowables as a result of the aging for both material systems. This decline should become more pronounced in the 10,000-hour results.

Differential Scanning Calorimetry

- No significant change in glass transition temperature was observed as a result of the aging. A broadening of the IM7/PETI-5 transition after 3000 hours of aging was observed in both stressed and unstressed samples. The broadening was attributed to physical aging effects that would restrict polymer chain movement.
- In all of the DSC tests runs, the first scan produced a lower glass transition temperature than the second scan. The lower glass transition temperature present in the second scan was believed to be the result of laminate processing effects which increased the free volume present in the polymer.

Thermogravimetric Analysis

- Results of the TGA showed a difference in weight loss rate for the different age IM7/K3B samples. The maximum rate of degradation for the first event decreased and shifted to lower temperatures for the aged material. Due to significant variations in

the measurements from sample to sample, more tests need to be run before more definite conclusion can be drawn.

- The IM7/PETI-5 composite didn't show any observable pattern between the weight loss rate curves for different aging times. This may suggest better thermal stability of the PETI-5 polymer over K3B.

Future Recommendations

Several questions still remain unanswered by this study. This next section will investigate some important issues that would increase our understanding of aging in composite material systems under stress and need further consideration.

- Many questions developed as to why the compressive strain in the aging panels, as measured by the strain gages, progressively declined. Most of the problem was attributed to creep of the strain gages, while different aging rates between the compressed panels and the thermal compensation panels and the viscoelastic nature of the panels were also considered. Moiré diffraction is currently being experimented using the 10,000-hour panels. The diffraction gratings were bonded to both exposed edges of the remaining eight compressed panels at the end of the 3000-hour period. At temperature, a replica of the grating is made and then viewed in an interferometer. With aging, if the actual strain in the panel changes, this method will provide a quantitative measurement of how much it changed. This technique significantly reduces the amount of unknowns involved in the strain measurement.
- The other significant question mentioned concerning the strain readings was the potential difference in strain due to aging between the material systems. Several unstressed composites and unstressed steel have been strain gaged in the same manner

as described in this report. Moiré gratings will be applied to all of the specimens. The strain gages will be measured separately so that any change in the strain due to aging can be observed and compared to the corresponding moiré reading. This will provide some measure of the strain change due to aging and of the strain change difference between IM7/K3B and IM7/PETI-5. Ideas are also being considered for monitoring the change in strain of a stressed specimen with both moiré gratings and strain gages adhered to it.

- Of course further study at longer aging times needs to be completed. Stressed panels have already been aging for over 3000 hours. Maybe after 10,000 hours some significant change in the strength values will be observed.
- The glass transition regions, as measured by DSC, were very weak due to the small amount of resin in each sample. Crushing of the composite sample, prior to crimping, may increase the area of contact between the pan and sample and also allow a larger amount of sample to be sealed in each pan. More samples also need to be run in order to determine how repeatable the measured values are. Other methods of obtaining glass transition temperature such as dynamic mechanical and dielectric could also be used to try and confirm the DSC results.
- TGA showed some promising results. There appeared to be a definite difference in weight loss rate for the IM7/K3B material as a result of the aging. The actual chemical differences between the unaged and aged TGA scans are still unknown. TGA mass spectroscopy would be able to detect the actual products that are given off at the different temperatures. These results would be useful in designing new polymers with better high temperature thermal stability. TGA might also provide a connection between changing chemical structure of the polymer matrix and declining mechanical properties at longer aging times.
- Modeling of the TGA results using a technique similar to Cunningham [28] could be useful in quantitatively comparing the different aging conditions. A TGA model could also help to associate changes in statistical strength to changes in degradation rate.

REFERENCES

1. Jones, Robert M., *Mechanics of Composite Materials*. Washington: Hemisphere Publishing Corporation, 1975 pp. 22-29.
2. Velicki, Alex, "Materials and Structures for the HSCT." *Aerospace Engineering*, 14 (April 1995), pp. 17-19.
3. Hutchinson, John M., "Physical Aging of Polymers." *Progress In Polymer Science*, 20 (1995) pp. 703-760.
4. Struik, L. C. E., "Physical Aging in Plastics and Other Glassy Materials." *Polymer Engineering and Science*, 17 (March 1977), pp. 165-173.
5. McKenna, Gregory B., "Glass Formation and Glassy Behavior." *Comprehensive Polymer Science*. New York: Pergamon Press, 1992 pp. 311-362.
6. Parvatareddy, H., Wang, J. Z., Dillard, D. A., Ward, T. C., and Rogalski, M. E., "Environmental Aging of High-Performance Polymeric Composites: Effects on Durability." *Composites Science and Technology*, 53 (1995), pp. 399-409.
7. Emanuel, N. M. and Buchachenko, A. L., *Chemical Physics of Polymer Degradation and Stabilization*. The Netherlands: VNU Science Press, 1987.
8. Davis, Anthony and Sims, D., *Weathering of Polymers*. New York: Applied Science Publishers LTD., 1983.
9. Bowels, Kenneth J., Roberts, G. D., and Kamvouris, J. E., "Long-Term Isothermal Aging Effects on Carbon Fabric-Reinforced PMR-15 Composites: Compression Strength." *2nd Symposium on High Temperature and Environmental Effects on Polymer Composites*, (submitted for publication).
10. Kerr, J. R. and Haskins, J. F., "Effects of 50,000 h of Thermal Aging on Graphite/Epoxy and Graphite/Polyimide Composites." *AIAA Journal*, 22 (January 1984), pp. 96-102.

11. G'Sell, Christian and McKenna, G. B., "Influence of Physical Aging on the Yield Response of Model DGEBA and Poly(propylene oxide) epoxy glasses." *Polymer*, 33 (1992), No. 10.
12. Mijovic, Jovan, "Interplay of Physical and Chemical Aging in Graphite/Epoxy Composites." *Journal of Composite Materials*, 19 (March 1985), pp. 178-191.
13. Lee, Andre and McKenna, G. B., "Effect of Crosslink Density on Physical Ageing of Epoxy Networks." *Polymer*, 29 (1988), pp. 1812-1817.
14. Sullivan, J. L., Blais, E. J., and Houston, D., "Physical Aging in the Creep Behavior of Thermosetting and Thermoplastic Composites." *Composites Science and Technology*, 40 (1993), pp. 389-403.
15. Struik, L. C. E., "The Mechanical and Physical Ageing of Semicrystalline Polymers: 1." *Polymer*, 28 (1987), pp. 1521-1533.
16. Hodge, Ian M., "Physical Aging in Polymer Glasses." *Science*, 267 (31 March 1995), pp. 1945-1947.
17. Ma, Chen-Chi M., et al., "Effect of Physical Aging on the Toughness of Carbon Fiber-Reinforced Poly(ether ether ketone) and Poly(phenylene sulfide) Composites. I." *Polymer Composites*, 13 (December 1992), pp. 441-447.
18. Gates, T. S. and Feldman, M., "Time-Dependent Behavior of a Graphite/Thermoplastic Composite and the Effects of Stress and Physical Aging." *Journal of Composites Technology and Research*, 17 (January 1995), pp. 33-42.
19. Sullivan, J. L., "Creep and Physical Aging of Composites." *Composites Science and Technology*, 39 (1990), pp. 207-232.
20. Dean, G. D., Read, B. E., and Tomlins, P. E., "A Model for Long-Term Creep and the Effects of Physical Ageing in Poly(butylene terephthalate)." *Plastics and Rubber Processing and Applications*, 13 (1990), pp. 37-46.
21. Peng, S. T. J., "Constitutive Equations of Ageing Polymeric Materials." *Journal of Materials Science*, 20 (1985), pp. 1920-1928.
22. Seitz, J. T., "The Estimation of Mechanical Properties of Polymers from Molecular Structure." *Journal of Applied Polymer Science*, 49 (1993), pp. 1331-1351.
23. Bair, Harvey E., "Glass Transition Measurements by DSC." *ASTM Special Technical Publication*, No. 1249 (1994), pp. 50-74.
24. Berens, Alan R. and Hodge, I. M., "Effects of Annealing and Prior History on Enthalpy Relaxation in Glassy Polymers. 1. Experimental Study on Poly(vinyl chloride)." *Macromolecules*, 15 (1982), pp. 756-761.
25. Hodge, Ian M. and Berens, A. R., "Effects of Annealing and Prior History on Enthalpy Relaxation in Glassy Polymers. 2. Mathematical Modeling." *Macromolecules*, 15 (1982), pp. 762-770.
26. Echeverria, Isabel, et al., "Physical Aging of a Polyetherimide: Creep and DSC Measurements." *Journal of Polymer Science: Part B: Polymer Physics*, 33 (1995), pp. 2457-2468.
27. Hinkley, J. A. and Jensen, B. J., "The Relative Thermooxidative Stability of a Phthalimide Against a Phenylethynylphthalimide Terminated Polyimide." *High Performance Polymers*, 1995 pp. 1-9.

28. Cunningham, Ronan., "Model-Driven Investigation of Environmental Degradation." Va Tech - MIT Student Symposium on Composite Materials, (25-26 March 1996).
29. Lin, S. C. and Pearce, E. M., "Epoxy Resins. I. The Stability of the Epoxy-Trimethoxyboroxine System." *Journal of Applied Polymer Science*, 23 (1979), pp. 3355-3374.
30. Lahrman, David F. et al., "Investigation of Scatter." The Boeing Company. Internal Report, (15 February 1995).
31. Berg, J. S. and Adams, D. F., "An Evaluation of Composite Material Compression Test Methods." *Journal of Composites Technology and Research*, 11 (Summer 1989), pp. 41-46.
32. Poon, C., R. Lee and Scott, R. F., "Compression Testing of Advanced Composite Laminates." *34th International SAMPE Symposium*, Vol. 34, pt. 2 (1989), pp. 2498-2505.
33. Whitney, James M. and Guihard, S. K., "Failure Modes in Compression Testing of Composite Materials." *36th International SAMPE Symposium and Exhibition*, Vol 36, pt. 1 (1991), pp. 1069-1078.
34. Daniels, J. A. and Sandhu, R. S., "Evaluation of Compression Specimens and Fixtures for Testing Unidirectional Composite Laminates." *ASTM Special Technical Publication*, No. 1206 (1993), pp. 103-123.
35. Odom, E. M. and Adams, D. F., "Failure Modes of Unidirectional Carbon/Epoxy Composite Compression Specimens." *Composites*, 21 (July 1990), pp. 289-296.
36. Herculac Incorporated, Product Data for Hercules Carbon Fiber Type IM7.
37. Wedgewood, Alan R., "Melt Processible Polyimides for High Performance Composite Applications." *24th International SAMPE Technical Conference*, 24 (October 1992), pp. T385-T398.
38. Hergenrother, P. M. and Smith, G. J., "Chemistry and Properties of Imide Oligomers End-capped with Phenylethynylphthalic Anhydrides." *Polymer*, 35 (1994), pp. 4857-4864.
39. ASTM Standard D3410/D3410M-94, "Standard Test Method for Compressive Properties of Polymer Matrix Composite Materials with Unsupported Gage Section by Shear Loading." *Annual Book of ASTM Standards*, Vol. 08.01, 1994, pp. 131-147.
40. Shay, W. M., 1990 "Strain-gage Stability Measurements for Three Years at 150°C in Air." *Experimental Mechanics*. pp. 158-163.
41. Daniel, W. M., *Applied Nonparametric Statistics*. Boston: PWS-KENT Publishing Company, 1978.
42. MIL-HDBK-17, Volume 1D-Guidelines, Department of Defense, Washington D.C. 20025, 1994.
43. Revised Test Plan for the Assessment of Residual Composite Properties as Influenced by Thermal Aging. submitted to The Boeing Company in 1996.
44. Test Fixture Documentation for HSR-II Component Structures Subtask 16.5.

APPENDIX A

Panel-Fixture Thermal Expansion Model¹

Nomenclature:

A = cross-sectional area,

l = axial dimension,

T = temperature,

α = coefficient of thermal expansion,

ε = axial strain,

σ = axial stress

$()_e$ = property of the end-plates in the fixture

$()_p$ = property of the composite panel

$()_r$ = property of the reaction rods in the fixture)

¹ The panel-fixture thermal expansion model was taken directly from this projects' test plan [43].

The changes in strain in the panel and in the fixture as the temperature increases from ambient, T_1 , to the required level for aging, T_2 , are given by,

$$\Delta \epsilon_p = \frac{\Delta \sigma_p}{E_p} + \alpha_p \Delta T \quad (A1)$$

$$\Delta \epsilon_f = \frac{\Delta \sigma_f}{E_f} + \alpha_f \Delta T \quad (A2)$$

The equilibrium of the panel-fixture assembly requires, α

$$\Delta \sigma_p A_p^{(2)} + \Delta \sigma_f A_f^{(2)} = 0 \quad (A3)$$

Note that $A_f^{(2)}$ represents the total cross-sectional area of the four reaction rods in the fixture. The cross-sectional areas of the panel and the reaction rods at T_2 are given by,

$$A_p^{(2)} = A_p^{(1)} (1 + 2\alpha_p) \Delta T \quad (A4)$$

$$A_f^{(2)} = A_f^{(1)} (1 + 2\alpha_f) \Delta T \quad (A5)$$

By eliminating $\Delta \sigma_p$ and $\Delta \sigma_f$ using Equations a1 and a2, and expressing $A_p^{(2)}$ and $A_f^{(2)}$ in terms of $A_p^{(1)}$ and $A_f^{(1)}$ using Equations a4 and a5, Equation a3 becomes,

$$\begin{aligned} E_p (\Delta \epsilon_p - \alpha_p \Delta T) A_p^{(1)} (1 + 2\alpha_p) \Delta T + \\ E_f (\Delta \epsilon_f - \alpha_f \Delta T) A_f^{(1)} (1 + 2\alpha_f) \Delta T = 0 \end{aligned} \quad (A6)$$

Compatibility between the panel and the fixture implies,

$$\Delta \epsilon_p l_p + 2\alpha_e l_e \Delta T = \Delta \epsilon_f (l_p + 2l_e) \quad (A7)$$

After rearranging, Equation a7 becomes,

$$\Delta \epsilon_f = m \Delta \epsilon_p + c \Delta T \quad (A8)$$

where

$$m = \left(1 + 2 \frac{l_e}{l_p} \right)^{-1} \quad (A9)$$

$$c = 2\alpha_e \frac{l_e}{l_p} \left(1 + 2 \frac{l_e}{l_p} \right)^{-1} \quad (A10)$$

Substituting Equation a8 into a6 and rearranging,

$$\Delta \epsilon_p = \frac{\alpha_p E_p (1 + 2\alpha_p) A_p^{(1)} + (\alpha_f - c) E_f (1 + 2\alpha_f) A_f^{(1)}}{E_p (1 + 2\alpha_p) A_p^{(1)} + m E_f (1 + 2\alpha_f) A_f^{(1)}} \Delta T \quad (A11)$$

By neglecting the change in cross-sectional area of the reaction rods and of the composite panel, it can be shown that Equation a11 is consistent with the corresponding expression given in Reference [44].

Weibull Equations

- Mean

$$\mu = \beta \Gamma\left(\frac{\alpha + 1}{\alpha}\right) \quad (\text{A12})$$

- Standard Deviation

$$\sigma = \left\{ \beta^2 \left[\Gamma\left(\frac{\alpha + 2}{\alpha}\right) - \Gamma^2\left(\frac{\alpha + 1}{\alpha}\right) \right] \right\}^{1/2} \quad (\text{A13})$$

- Shape Parameter (α)

– Alpha is the slope of the Cumulative Percent Occurred versus Property (Strength or Modulus) plot.

- Characteristic Value (β)

– Beta is the x-intercept of the Cumulative Percent Occurred versus Property (Strength or Modulus) plot.

- Allowables

$$\text{A or B-basis allowable} = \tilde{\beta} \left(\ln \frac{1}{R} \right)^{1/\alpha} \quad (\text{A14})$$

$$\tilde{\beta} = \beta \left[\frac{2n}{X_{CL}^2(2n)} \right]^{1/\alpha} \quad (\text{A15})$$

X_{CL}^2 = Chi-square function for a given confidence level (lower bound)

n = Number of samples in the population

R = Reliability

VITA

Richard B. Plunkett was born on July 13, 1973 to Mary W. and Richard C. Plunkett in Philadelphia, PA. He grew up in the suburbs just west of Philadelphia. Rich graduated from Upper Moreland High School in the spring of 1991 and proceeded to attend Virginia Polytechnic Institute the following fall. Mr. Plunkett graduated with a Bachelor of Science degree from the Engineering Science and Mechanics department in May of 1995. While studying engineering at Virginia Tech, Rich spent his summers and free time working in the composite materials laboratory performing various research tasks. In the summer after graduation, he was accepted to the Engineering Mechanics program at Virginia Tech and was awarded both graduate and research assistantships. One year later in October of 1996, Rich graduated with a master of science degree from the Engineering Science and Mechanics department.

Richard B. Plunkett